Jin-Gen Dai, Cheng-Shan Wang, Robert J. Stern, Kai Yang, and Jie Shen, 2020, Forearc magmatic evolution during subduction initiation: Insights from an Early Cretaceous Tibetan ophiolite and comparison with the Izu-Bonin-Mariana forearc: GSA Bulletin, https://doi.org/10.1130/B35644.1.

Supplemental Material

Text S1. Analytical Methods

Table S1. Major and Trace elements of the clinopyroxene from the gabbroic pegmatite in the Xigaze Ophiolite.

Table S2. Major and Trace elements of the orthopyroxene from the gabbroic pegmatite and the plagiogranite in the Xigaze Ophiolite.

Table S3. Major and Trace elements of the amphibole from the gabbroic pegmatite and the plagiogranite in the Xigaze Ophiolite.

Table S4. Whole rock analyses of clinopyroxene megacryst, gabbroic pegmatite, plagiogranite, basaltic and diabase dike/enclave, pillow basalt.

Table S5. Whole-rock Sr-Nd isotopes of gabbroic pegmatite and plagiogranite in the Xigaze Ophiolite.

Table S6. LA-ICP-MS U-Pb data for zircon from plagiogranite in the Xigaze Ophiolite.

Table S7. LA-ICP-MS Lu-Hf data for zircon from plagiogranite in the Xigaze Ophiolite.

Figure S1. (A) Classification of pyroxenes from the Xigaze gabbroic pegmatite and plagiogranite in the system of Wo ($Ca_2Si_2O_6$), En ($Mg_2Si_2O_6$), and Fs ($Fe_2Si_2O_6$). (B) Composition of amphiboles from the Xigaze gabbroic pegmatite and plagiogranite (Leake et al., 1997). Two amphiboles from plagiogranite plot in the field of ferro-actinolite (not shown here).

Figure S2. Major element compositions of clinopyroxenes (A-C) and amphiboles (D-F) from the Xigaze gabbroic pegmatite and plagiogranite. Mg# versus Cr_2O_3 (A), Al_2O_3 (B), and TiO_2 (C); Al_2O_3 versus SiO_2 (D), TiO_2 (E), Na_2O (F). The compared clinopyroxenes of the diabase and basalt are from Dubois-Côté et al. (2005); Hébert et al. (2003); clinopyroxenes of gabbro from Liu et al. (2018). Cpx—clinopyroxene; Amp—amphibole.

Figure S3. Major element variations of mafic rocks and plagiogranites in the Xigaze Ophiolite. Data of mafic rocks of the Xigaze Ophiolite are from Bao et al. (2013); Chen and Xia (2008); Dubois-Côté et al. (2005); Malpas et al. (2003); Li et al. (2012); Niu et al. (2006); L. Zhang et al. (2016); Data of plagiogranites are from L. Zhang et al. (2016).

Figure S4. Trace element-SiO_2 variations for mafic rocks to plagiogranites in the Xigaze Ophiolite. Data sources are the same with those of Figure S3.

Figure S5. (A) Feldspar normative An–Ab–Or diagram of plagiogranites in the Xigaze Ophiolite. The field of oceanic plagiogranites is from Coleman and Peterman (1975). (B) TiO_2 versus SiO_2 of the Xigaze plagiogranite. The dotted line represents the minimum TiO_2 values of SiO_2–enriched melt generated by differentiation of a MORB–tholeiitic parental magma. Field of ophiolitic plagiogranite and melt generated by anatexis of gabbroic rocks are from Koepke et al. (2007).

INTRODUCTION

Data repository contains full details of analytical methods for mineral chemistry, whole-rock geochemical analysis, zircon U-Pb analysis. In addition, sources of compiled data are also listed. Analytical results for major and trace elements of clinopyroxene (Table S1), orthopyroxene (Table S2), amphibole (Table S3); whole rock analyses of clinopyroxene megacryst, gabbroic pegmatite, plagiogranite, basaltic and diabase dike/enclave, pillow basalt (Tables S4 and S5); zircon U-Pb ages (Table S6) and Lu-Hf isotopic composition (Table S7). All references cited in the Data Repository are listed in the main text.

TEXT S1 ANALYTICAL METHODS

Mineral Chemistry

The major element compositions of minerals were determined using a JXA-8100 electron microprobe at the Analytical Laboratory of the Beijing Research Institute of Uranium Geology. The analytical conditions were as follows: an acceleration voltage of 20 kV, a beam current of 10 nA, a beam diameter of 2 μm, and counting times of 10–30 s for peaks and 10 s for background for each element. The measured data were corrected by the ZAF method. The relative analytical accuracy was better than 1%.

In situ trace element analyses of clinopyroxene, orthopyroxene and amphibole were conducted at the Key Laboratory of Continental Dynamics, Northwest University using an Agilent 7500a ICP-MS coupled to a GeoLas 200M laser ablation system. Each analysis was performed by ablating a 30-μm diameter spot at 5 Hz. Calibration was performed using NIST SRM 610 as the external standard in conjunction with internal standardization using Ca measured by electron microprobe. The data were reduced using the GLITTER 4.0 software. Analyses of USGS basalt glass standards GSE-1G, BCR-2G and BHVO-2G demonstrated analytical precision and accuracy better than 5%. The analytical procedures followed those described by S. Gao et al. (2002). Major and trace elements of clinopyroxene, orthopyroxene, and amphibole are shown in Tables S1, S2, S3, respectively.

Whole-rock Geochemistry

Samples were powdered to less than 200-mesh size for whole-rock analyses. Two clinopyroxene megacrysts, two gabbroic pegmatites and three plagiogranites were analyzed. Major element analyses were performed using a SHIMADZU XRF-1800 spectrometer by the X-ray fluorescence (XRF) method in fused glass disks at the State Key Laboratory of Geological Processes and Mineral Resources, China University of Geosciences, Beijing. The accuracy for the analytical results was typically 2%–5%.

Whole-rock trace element compositions were determined by a Finnigan MAT Element II ICP-MS at the State Key Laboratory of Mineral Deposits Research, Nanjing University. Samples were dissolved by a mixture of HF and HNO_3 in Teflon digesting vessels on a hot plate for 24 h. This procedure was repeated using smaller amounts of acids for 12 h. After digestion, samples were dried, refluxed with 6 N HNO_3, and heated again to incipient dryness. The USGS reference materials (W-2 and AGV-2) were used to monitor the analytical accuracy. The results indicated that the accuracy was better than 10% for most elements, with many elements agreeing to within

2% of the recommended values (Tables S4). Analytical details were described by J. Gao et al. (2003).

Sr and Nd isotopic analyses were performed at the Tianjin Institute of Geology and Mineral Resources, China Geological Survey. Samples were digested with acids digestion HNO_3 and HF. The separation of Rb, Sr and light REE was accomplished through a cation-exchange column. Sm and Nd were further purified using a second cation-exchange column, and were conditioned and cleaned with dilute HCl. Sr-Nd isotope ratios were measured on a negative thermal ionization mass spectrometer (NTIMS) by TRITON. Measured $^{87}Sr/^{86}Sr$ and $^{143}Nd/^{144}Nd$ ratios were corrected for mass fractionation with $^{86}Sr/^{88}Sr = 0.1194$ and $^{146}Nd/^{144}Nd = 0.7219$. During the analytical sessions, NBS-987 $SrCO_3$ Sr standard ($^{87}Sr/^{86}Sr = 0.710250$) and JMC Nd_2O_3 Nd standard ($^{143}Nd/^{144}Nd = 0.511122$) were run to monitor the equipment. Sr-Nd isotopic data are listed in Table S5.

LA-ICP-MS Zircon U-Pb Dating

U-Pb zircon dating was performed on one representative plagiogranite sample (DJG13–52). Zircon concentrates were obtained using standard density and magnetic separation techniques. Individual crystals were handpicked and mounted in epoxy resin. Cathodoluminescence images were used to check the internal structures of individual zircon grains and to select positions for analyses. U-Pb dating of zircon was performed by laser ablation inductively coupled plasma mass spectrometry (LA-ICP-MS) at the State Key Laboratory of Mineral Deposit Research, Nanjing University, China, following the method described by Jackson et al. (2004). The laser-ablation spot diameter was 25 μm. The off–line isotope ratios and trace element concentrations were calculated by GLITTER 4.0. The common Pb correction and ages of the samples were calibrated and calculated using ComPbCorr#3.15 (Andersen, 2002). The U-Pb concordia diagrams, weighted mean calculations and probability density plots of U-Pb ages were made using Isoplot 3.6 (Ludwig, 2008). Zircon U-Pb ages are given in Table S6.

Zircon Lu-Hf Analysis

In situ zircon Lu-Hf isotope (Sample DJ12–17 and DJ12–19) were determined on a Neptune Multi-Collector ICP-MS (MC-ICP-MS) equipped with a Geolas-193 laser-ablation system at the Institute of Geology and Geophysics, Chinese Academy of Sciences, Beijing. These analyses were performed on the dated spots of each zircon grain. The diameters of laser ablated spots were 40 μm for both samples, which were larger than that of pre-existing spots (25 μm) produced by U-Pb dating. Instrumental conditions and data acquisition were similar to those described by Wu et al. (2006). Measured $^{176}Hf/^{177}Hf$ ratios were normalized to $^{179}Hf/^{177}Hf = 0.7325$. The $\varepsilon_{Hf}(t)$ values and T_{DM} were calculated following Griffin et al. (2000) using the ^{176}Lu decay constant given in Blichert-Toft and Albarède (1997). The zircon Hf isotope data are listed in Table S7.

Sources of Compiled Data

Abundant mineral and whole-rock geochemical, geochronological data have been published for the Yarlung Zangbo Ophiolite (YZO). Previous studies have compiled data for the entire YZO (cf. Hébert et al., 2012). Given that the complexity and variability along the strike of the YZO, here we just compiled data from the Xigaze Ophiolite. The following data sets have been compiled: (1) Mineral geochemical data: Clinopyroxene major elements of diabase and basalt from Dubois-Côté et al. (2005); Hébert et al. (2003); while clinopyroxene of gabbro from Liu et al. (2018). Clinopyroxene trace element of gabbroic dikes in the Oman Ophiolite and the Xigaze Ophiolite from Yamasaki et al. (2006) and Koepke et al. (2009), and Liu et al. (2018), respectively. (2) Whole-rock geochemical data: plagiogranite from L. Zhang et al. (2016); basalt from Bao et al. (2013); Chen and Xia (2008); Dubois–Côté et al. (2005); Malpas et al. (2003); Li et al. (2012); Niu et al. (2006); L. Zhang et al. (2016); IBM forearc basalt from Ishizuka et al. (2011, 2018); Reagan et al. (2010, 2017). (3) Zircon U-Pb ages: mafic rock and plagiogranite of the Xigaze Ophiolite from Dai et al. (2013); Liu et al. (2016); L. Zhang et al. (2016); Gangdese arc from Chu et al. (2011); Guan et al. (2012); Guo et al. (2013); Huang et al. (2016); Ji et al. (2009, 2012); Ma et al. (2013); Pan et al. (2016); Wang et al. (2015); B. Xu et al. (2017); W. Xu et al. (2015); Yang et al. (2016); Zhang et al. (2010); Zhu et al. (2011). (4) Lithology and ages of the Xigaze Forearc Basin (XFB) from Dai et al. (2015); J. Wang et al. (2017); Wang et al. (2012); Wu et al. (2010).

REFERENCES CITED

Andersen, T., 2002, Correction of common lead in U–Pb analyses that do not report 204Pb: Chemical Geology, v. 192, no. 1–2, p. 59–79, https://doi.org/10.1016/S0009-2541(02)00195-X.

Bao, P.S., Su, L., Wang, J., and Zhai, Q.G., 2013, Study on the Tectonic Setting for the Ophiolites in Xigaze, Tibet: Acta Geologica Sinica-English Edition, v. 87, no. 2, p. 395–425, https://doi.org/10.1111/1755-6724.12058.

Blichert-Toft, J., and Albarède, F., 1997, The Lu-Hf isotope geochemistry of chondrites and the evolution of the mantle-crust system: Earth and Planetary Science Letters, v. 148, no. 1, p. 243–258, https://doi.org/10.1016/S0012-821X(97)00040-X.

Chen, G.W., and Xia, B., 2008, Platinum-group elemental geochemistry of mafic and ultramafic rocks from the Xigaze ophiolite, southern Tibet: Journal of Asian Earth Sciences, v. 32, no. 5–6, p. 406–422, https://doi.org/10.1016/j.jseaes.2007.11.009.

Chu, M.F., Chung, S.-L., O'Reilly, S.Y., Pearson, N.J., Wu, F.-Y., Li, X.-H., Liu, D., Ji, J., Chu, C.-H., and Lee, H.-Y., 2011, India's hidden inputs to Tibetan orogeny revealed by Hf isotopes of Transhimalayan zircons and host rocks: Earth and Planetary Science Letters, v. 307, no. 3–4, p. 479–486, https://doi.org/10.1016/j.epsl.2011.05.020.

Coleman, R.G., and Peterman, Z.E., 1975, Oceanic plagiogranite: Journal of Geophysical Research, v. 80, no. 8, p. 1099–1108, https://doi.org/10.1029/JB080i008p01099.

Dai, J., Wang, C., Polat, A., Santosh, M., Li, Y., and Ge, Y., 2013, Rapid forearc spreading between 130 and 120 Ma: Evidence from geochronology and geochemistry of the Xigaze ophiolite, southern Tibet: Lithos, v. 172–173, no. 0, p. 1–16, https://doi.org/10.1016/j.lithos.2013.03.011.

Dai, J.G., Wang, C.S., Zhu, D.C., Li, Y.L., Zhong, H.T., and Ge, Y.K., 2015, Multi-stage volcanic activities and geodynamic evolution of the Lhasa terrane during the Cretaceous: Insights from the Xigaze forearc basin: Lithos, v. 218, p. 127–140, https://doi.org/10.1016/j.lithos.2015.01.019.

Dubois-Côté, V., Hébert, R., Dupuis, C., Wang, C.S., Li, Y.L., and Dostal, J., 2005, Petrological and geochemical evidence for the origin of the Yarlung Zangbo ophiolites, southern Tibet: Chemical Geology, v. 214, no. 3–4, p. 265–286, https://doi.org/10.1016/j.chemgeo.2004.10.004.

Gao, J.F., Lu, J.J., Lai, M.Y., Lin, Y.P., and Pu, W., 2003, Analysis of trace elements in rock samples using HR-ICPMS [Natural Sciences]: Journal of Nanjing University, v. 39, p. 844–850.

Gao, S., Liu, X., Yuan, H., Hattendorf, B., Günther, D., Chen, L., and Hu, S., 2002, Determination of Forty Two Major and Trace Elements in USGS and NIST SRM Glasses by Laser Ablation-Inductively Coupled Plasma-Mass Spectrometry: Geostandards Newsletter, v. 26, no. 2, p. 181–196, https://doi.org/10.1111/j.1751-908X.2002.tb00886.x.

Griffin, W.L., Pearson, N.J., Belousova, E., Jackson, S.E., van Achterbergh, E., O'Reilly, S.Y., and Shee, S.R., 2000, The Hf isotope composition of cratonic mantle: LAM-MC-ICPMS analysis of zircon megacrysts in kimberlites: Geochimica et Cosmochimica Acta, v. 64, no. 1, p. 133–147, https://doi.org/10.1016/S0016-7037(99)00343-9.

Guan, Q., Zhu, D.C., Zhao, Z.D., Dong, G.C., Zhang, L.L., Li, X.W., Liu, M., Mo, X.X., Liu, Y.S., and Yuan, H.L., 2012, Crustal thickening prior to 38 Ma in southern Tibet: Evidence from lower crust-derived adakitic magmatism in the Gangdese Batholith: Gondwana Research, v. 21, no. 1, p. 88–99, https://doi.org/10.1016/j.gr.2011.07.004.

Guo, L., Zhang, H.-F., Harris, N., Pan, F.-B., and Xu, W.-C., 2013, Late Cretaceous (~81Ma) high-temperature metamorphism in the southeastern Lhasa terrane: Implication for the Neo-Tethys ocean ridge subduction: Tectonophysics, v. 608, p. 112–126, https://doi.org/10.1016/j.tecto.2013.10.007.

Hébert, R., Bezard, R., Guilmette, C., Dostal, J., Wang, C.S., and Liu, Z.F., 2012, The Indus–Yarlung Zangbo ophiolites from Nanga Parbat to Namche Barwa syntaxes, southern Tibet: First synthesis of petrology, geochemistry, and geochronology with incidences on geodynamic reconstructions of Neo-Tethys: Gondwana Research, v. 22, no. 2, p. 377–397, https://doi.org/10.1016/j.gr.2011.10.013.

Hébert, R., Huot, F., Wang, C.S., and Liu, Z.F., 2003, Yarlung Zangbo ophiolites (Southern Tibet) revisited: geodynamic implications from the mineral record, *in* Dilek, Y., and Robinson, P.T., eds., Ophiolites in Earth History. Geological Society, London, Special Publications, v. 218, p. 165–190, https://doi.org/10.1144/GSL.SP.2003.218.01.10.

Huang, F., Xu, J.-F., Chen, J.-L., Wu, J.-B., Zeng, Y.-C., Xiong, Q.-W., Chen, X.-F., and Yu, H.-X., 2016, Two Cenozoic tectonic events of N–S and E–W extension in the Lhasa Terrane: Evidence from geology and geochronology: Lithos, v. 245, p. 118–132, https://doi.org/10.1016/j.lithos.2015.08.014.

Ishizuka, O., Hickey-Vargas, R., Arculus, R.J., Yogodzinski, G.M., Savov, I.P., Kusano, Y., McCarthy, A., Brandl, P.A., and Sudo, M., 2018, Age of Izu–Bonin–Mariana arc basement: Earth and Planetary Science Letters, v. 481, p. 80–90, https://doi.org/10.1016/j.epsl.2017.10.023.

Ishizuka, O., Tani, K., Reagan, M.K., Kanayama, K., Umino, S., Harigane, Y., Sakamoto, I., Miyajima, Y., Yuasa, M., and Dunkley, D.J., 2011, The timescales of subduction initiation and subsequent evolution of an oceanic island arc: Earth and Planetary Science Letters, v. 306, no. 3–4, p. 229–240, https://doi.org/10.1016/j.epsl.2011.04.006.

Jackson, S.E., Pearson, N.J., Griffin, W.L., and Belousova, E.A., 2004, The application of laser ablation-inductively coupled plasma-mass spectrometry to in situ U-Pb zircon

geochronology: Chemical Geology, v. 211, no. 1–2, p. 47–69, https://doi.org/10.1016/j.chemgeo.2004.06.017.
Ji, W.-Q., Wu, F.-Y., Chung, S.-L., Li, J.-X., and Liu, C.-Z., 2009, Zircon U-Pb geochronology and Hf isotopic constraints on petrogenesis of the Gangdese batholith, southern Tibet: Chemical Geology, v. 262, no. 3–4, p. 229–245, https://doi.org/10.1016/j.chemgeo.2009.01.020.
Ji, W.Q., Wu, F.Y., Liu, C.Z., and Chung, S.L., 2012, Early Eocene crustal thickening in southern Tibet: New age and geochemical constraints from the Gangdese batholith: Journal of Asian Earth Sciences, v. 53, p. 82–95, https://doi.org/10.1016/j.jseaes.2011.08.020.
Koepke, J., Schoenborn, S., Oelze, M., Wittmann, H., Feig, S.T., Hellebrand, E., Boudier, F., and Schoenberg, R., 2009, Petrogenesis of crustal wehrlites in the Oman ophiolite: Experiments and natural rocks: Geochemistry Geophysics Geosystems, v. 10, no. 10, Q10002, https://doi.org/10.1029/2009GC002488.
Koepke, J., Berndt, J., Feig, S., and Holtz, F., 2007, The formation of SiO2-rich melts within the deep oceanic crust by hydrous partial melting of gabbros: Contributions to Mineralogy and Petrology, v. 153, no. 1, p. 67–84, https://doi.org/10.1007/s00410-006-0135-y.
Leake, B.E., Woolley, A.R., Kisch, H.J., Krivovichev, V.G., Linthout, K., Laird, J., Maresch, W.V., Schumacher, J.C., Stephenson, N.C., and Whittaker, E.J., 1997, Nomenclature of amphiboles: report of the subcommittee on amphiboles of the International Mineralogical Association, Commission on New Minerals and Mineral Names: Canadian Mineralogist, v. 35, p. 219–246.
Li, W.X., Zhao, Z.D., Zhu, D.C., Dung, G.C., Zhou, S., Mo, X.X., DePaolo, D., and Dilek, Y., 2012, Geochemical discrimination of tectonic environments of the Yalung Zangpo ophiolite in southern Tibet: Yanshi Xuebao, v. 28, no. 5, p. 1663–1673.
Liu, T., Wu, F.-Y., Liu, C.-Z., Tribuzio, R., Ji, W.-B., Zhang, C., Xu, Y., and Zhang, W.-Q., 2018, Variably evolved gabbroic intrusions within the Xigaze ophiolite (Tibet): new insights into the origin of ophiolite diversity: Contributions to Mineralogy and Petrology, v. 173, no. 11, p. 91, https://doi.org/10.1007/s00410-018-1518-6.
Liu, T., Wu, F.-Y., Zhang, L.-L., Zhai, Q.-G., Liu, C.-Z., Ji, W.-B., Zhang, C., and Xu, Y., 2016, Zircon U-Pb geochronological constraints on rapid exhumation of the mantle peridotite of the Xigaze ophiolite, southern Tibet: Chemical Geology, v. 443, p. 67–86, https://doi.org/10.1016/j.chemgeo.2016.09.015.
Ludwig, K.R., 2008, User's Manual for Isoplot 3.60: Berkeley Geochronology Center Special Publication, 4.
Ma, L., Wang, Q., Wyman, D.A., Li, Z.-X., Jiang, Z.-Q., Yang, J.-H., Gou, G.-N., and Guo, H.-F., 2013, Late Cretaceous (100–89 Ma) magnesian charnockites with adakitic affinities in the Milin area, eastern Gangdese: Partial melting of subducted oceanic crust and implications for crustal growth in southern Tibet: Lithos, v. 175–176, no. 0, p. 315–332, https://doi.org/10.1016/j.lithos.2013.04.006.
Malpas, J., Zhou, M.F., Robinson, P.T., and Reynolds, P.H., 2003, Geochemical and geochronological constraints on the origin and emplacement of the Yarlung Zangbo ophiolites, Southern Tibet, *in* Dilek, Y., and Robinson, P. T., eds., Ophiolites in Earth History, v. 218, p. 191–206, https://doi.org/10.1144/GSL.SP.2003.218.01.11.
Niu, X.L., Zhao, Z.D., Mo, X.X., Depaolo, D.J., Dong, G., Zhang, S.Q., Zhu, D.C., and Guo, T.Y., 2006, Elemental and Sr-Nd-Pb isotopic geochemistry for basic rocks from Decun-

Angren ophiolites in Xigaze area, Tibet: implications for the characteristics of the Tethyan upper mantle domain: Yanshi Xuebao, v. 22, no. 12, p. 2875–2888.
Pan, F.-B., Zhang, H.-F., Xu, W.-C., Guo, L., Luo, B.-J., and Wang, S., 2016, U–Pb zircon dating, geochemical and Sr–Nd–Hf isotopic compositions of Motuo quartz–monzonite: Implication for the genesis and diversity of the high Ba–Sr granitoids in orogenic belt: Tectonophysics, v. 668–669, p. 52–64, https://doi.org/10.1016/j.tecto.2015.12.007.
Reagan, M.K., Ishizuka, O., Stern, R.J., Kelley, K.A., Ohara, Y., Blichert-Toft, J., Bloomer, S.H., Cash, J., Fryer, P., Hanan, B.B., Hickey-Vargas, R., Ishii, T., Kimura, J.-I., Peate, D.W., Rowe, M.C., and Woods, M., 2010, Fore-arc basalts and subduction initiation in the Izu-Bonin-Mariana system: Geochemistry Geophysics Geosystems, v. 11, no. 3, Q03X12, https://doi.org/10.1029/2009GC002871.
Reagan, M.K., Pearce, J.A., Petronotis, K., Almeev, R.R., Avery, A.J., Carvallo, C., Chapman, T., Christeson, G.L., Ferré, E.C., Godard, M., Heaton, D.E., Kirchenbaur, M., Kurz, W., Kutterolf, S., Li, H., Li, Y., Michibayashi, K., Morgan, S., Nelson, W.R., Prytulak, J., Python, M., Robertson, A.H.F., Ryan, J.G., Sager, W.W., Sakuyama, T., Shervais, J.W., Shimizu, K., and Whattam, S.A., 2017, Subduction initiation and ophiolite crust: new insights from IODP drilling: International Geology Review, v. 59, no. 11, p. 1439–1450, https://doi.org/10.1080/00206814.2016.1276482.
Wang, C., Li, X., Liu, Z., Li, Y., Jansa, L., Dai, J., and Wei, Y., 2012, Revision of the Cretaceous–Paleogene stratigraphic framework, facies architecture and provenance of the Xigaze forearc basin along the Yarlung Zangbo suture zone: Gondwana Research, v. 22, no. 2, p. 415–433, https://doi.org/10.1016/j.gr.2011.09.014.
Wang, J.-G., Hu, X., Garzanti, E., An, W., and Liu, X.-C., 2017, The birth of the Xigaze forearc basin in southern Tibet: Earth and Planetary Science Letters, v. 465, p. 38–47, https://doi.org/10.1016/j.epsl.2017.02.036.
Wang, Q., Zhu, D.C., Cawood, P.A., Zhao, Z.D., Liu, S.A., Chung, S.L., Zhang, L.L., Liu, D., Zheng, Y.C., and Dai, J.G., 2015, Eocene magmatic processes and crustal thickening in southern Tibet: Insights from strongly fractionated ca. 43 Ma granites in the western Gangdese Batholith: Lithos, v. 239, p. 128–141, https://doi.org/10.1016/j.lithos.2015.10.003.
Wu, F.-Y., Yang, Y.-H., Xie, L.-W., Yang, J.-H., and Xu, P., 2006, Hf isotopic compositions of the standard zircons and baddeleyites used in U–Pb geochronology: Chemical Geology, v. 234, no. 1–2, p. 105–126, https://doi.org/10.1016/j.chemgeo.2006.05.003.
Wu, F.Y., Ji, W.Q., Liu, C.Z., and Chung, S.L., 2010, Detrital zircon U-Pb and Hf isotopic data from the Xigaze fore-arc basin: Constraints on Transhimalayan magmatic evolution in southern Tibet: Chemical Geology, v. 271, no. 1–2, p. 13–25, https://doi.org/10.1016/j.chemgeo.2009.12.007.
Xu, B., Hou, Z.-Q., Zheng, Y.-C., Wang, R., He, M.-Y., Zhou, L.-M., Wang, Z.-X., He, W.-Y., Zhou, Y., and Yang, Y., 2017, In situ elemental and isotopic study of diorite intrusions: Implication for Jurassic arc magmatism and porphyry Cu-Au mineralisation in southern Tibet: Ore Geology Reviews, v. 90, p. 1063–1077, https://doi.org/10.1016/j.oregeorev.2017.04.036.
Xu, W.-C., Zhang, H.-F., Luo, B.-j., Guo, L., and Yang, H., 2015, Adakite-like geochemical signature produced by amphibole-dominated fractionation of arc magmas: An example from the Late Cretaceous magmatism in Gangdese belt, south Tibet: Lithos, v. 232, p. 197–210, https://doi.org/10.1016/j.lithos.2015.07.001.

Yamasaki, T., Maeda, J., and Mizuta, T., 2006, Geochemical evidence in clinopyroxenes from gabbroic sequence for two distinct magmatisms in the Oman ophiolite: Earth and Planetary Science Letters, v. 251, no. 1–2, p. 52–65, https://doi.org/10.1016/j.epsl.2006.08.027.

Yang, Z., Hou, Z., Chang, Z., Li, Q., Liu, Y., Qu, H., Sun, M., and Xu, B., 2016, Cospatial Eocene and Miocene granitoids from the Jiru Cu deposit in Tibet: Petrogenesis and implications for the formation of collisional and postcollisional porphyry Cu systems in continental collision zones: Lithos, v. 245, p. 243–257, https://doi.org/10.1016/j.lithos.2015.04.002.

Zhang, H., Harris, N., Liang, G., and Xu, W., 2010, The significance of Cenozoic magmatism from the western margin of the eastern syntaxis, southeast Tibet: Contributions to Mineralogy and Petrology, v. 160, no. 1, p. 83–98, https://doi.org/10.1007/s00410-009-0467-5.

Zhang, L.-L., Liu, C.-Z., Wu, F.-Y., Zhang, C., Ji, W.-Q., and Wang, J.-G., 2016, Sr–Nd–Hf isotopes of the intrusive rocks in the Cretaceous Xigaze ophiolite, southern Tibet: Constraints on its formation setting: Lithos, v. 258–259, p. 133–148, https://doi.org/10.1016/j.lithos.2016.04.026.

Zhu, D.-C., Zhao, Z.-D., Niu, Y., Mo, X.-X., Chung, S.-L., Hou, Z.-Q., Wang, L.-Q., and Wu, F.-Y., 2011, The Lhasa Terrane: Record of a microcontinent and its histories of drift and growth: Earth and Planetary Science Letters, v. 301, no. 1–2, p. 241–255, https://doi.org/10.1016/j.epsl.2010.11.005.

In the supplementary tables, all the major elements and En, Fs, Wo are in wt%.

Table S1 Major and Trace elements of the clinopyroxene from the gabbroic pegmatite in the Xigaze Ophiolite

Sample	DJG13-45-2	DJG13-45-3	DJG13-45-4	DJG13-45-5	DJG13-45-14	DJG13-45-15	DJG13-45-16	DJG13-65-1
SiO_2	53.39	53.43	53.32	53.52	53.49	53.74	53.81	52.79
TiO_2	0.27	0.22	0.38	0.26	0.24	0.2	0.26	0.26
Al_2O_3	2.18	1.92	2.44	2.2	1.09	2.05	2.16	1.89
Cr_2O_3	0.06	0.19	0.08	0.06	0.05	0.08	0.2	
FeO	5.49	4.74	5.65	4.44	6.71	4.32	5.68	8.35
MnO	0.18	0.13	0.12	0.11	0.15	0.14	0.19	0.27
MgO	14.48	15.05	15.15	15.05	13.99	15.23	16.13	13.88
CaO	23.01	23.28	22.1	22.99	23.11	23.08	21.13	21.98
Na_2O	0.16	0.17	0.11	0.16	0.21	0.14	0.13	0.28
K_2O								
NiO		0.1	0.04					
Total	99.22	99.23	99.39	98.79	99.04	98.98	99.69	99.7
Si	1.9866	1.9813	1.9761	1.9907	2.0042	1.9940	1.9828	1.9696
Ti	0.0076	0.0061	0.0106	0.0073	0.0068	0.0056	0.0072	0.0073
Al	0.0956	0.0839	0.1066	0.0964	0.0481	0.0896	0.0938	0.0831
Cr	0.0018	0.0056	0.0023	0.0018	0.0015	0.0023	0.0058	0.0000
Fe^{3}	0.0000	0.0000	0.0000	0.0000	0.0000	0.0000	0.0000	0.0000
Fe^{2}	0.1708	0.1470	0.1751	0.1381	0.2102	0.1340	0.1750	0.2605
Fe	0.1708	0.1470	0.1751	0.1381	0.2102	0.1340	0.1750	0.2605
Mn	0.0057	0.0041	0.0038	0.0035	0.0048	0.0044	0.0059	0.0085
Mg	0.8032	0.8320	0.8371	0.8346	0.7815	0.8425	0.8861	0.7721
Ca	0.9172	0.9248	0.8775	0.9161	0.9277	0.9175	0.8341	0.8786
Na	0.0115	0.0122	0.0079	0.0115	0.0153	0.0101	0.0093	0.0203
K	0.0000	0.0000	0.0000	0.0000	0.0000	0.0000	0.0000	0.0000
Ni	0.0000	0.0030	0.0012	0.0000	0.0000	0.0000	0.0000	0.0000
Sum	4.0000	4.0000	3.9981	4.0000	4.0000	4.0000	4.0000	4.0000
Al(VI)	0.0897	0.0713	0.0933	0.0944	0.0591	0.0892	0.0838	0.0600
Al(IV)	0.0059	0.0126	0.0133	0.0020	0.0000	0.0004	0.0100	0.0231
En	42.34	43.61	44.21	44.10	40.61	44.38	46.61	40.22
Fs	9.30	7.92	9.45	7.48	11.17	7.29	9.52	14.02
Wo	48.35	48.47	46.34	48.41	48.21	48.33	43.87	45.77
Mg#	0.82	0.85	0.83	0.86	0.79	0.86	0.84	0.75
T(°C)*	1174	1177	1166	1183	1172	1177	1191	1182
Trace element (ppm)								
Li	0.756	1.532	0.906	1.011	1.444	0.949	0.894	1.334
Be				0.032	0.139	0.05		0.095
B	6.73	5.36	5.54	5.76	5.52	6.13	5.73	3.89
P	79.6	38.47	36.63	37.35	48.6	43.04	40.27	41.93
K	160.53	27.79	19.78	14.04	14.73	61.38	35.33	39.59
Sc	113.13	93.09	87.32	95.55	113	110	101	188
Ti	1681	760	1051	1118	1359	2110	1206	1887
V	496	345	330	348	382	393	362	705
Cr	1178	1137	983	1125	359	548	1091	11.89
Mn	2111	1067	1032	1141	1613	1510	1281	1935
Co	70.93	39.12	34.14	38.42	37.53	37.24	39.95	58.02
Ni	520	330	290	311	142	191	259	98.34
Cu	0.764	16.69	4.95	5.96	0.26	37.23	27.54	122.23
Zn	53.04	18.82	17.81	21.61	36.13	32.07	23.49	58.44
Ga	3.78	2.6	2.3	2.8	3.12	3.11	2.53	5.36

Sample	DJG13-45-2	DJG13-45-3	DJG13-45-4	DJG13-45-5	DJG13-45-14	DJG13-45-15	DJG13-45-16	DJG13-65-1
Ge	3.16	1.66	1.92	1.91	2.01	2.23	1.69	3.86
As		0.39		0.449	0.18	0.309		0.36
Rb	0.329		0.055			0.102	0.108	0.146
Sr	8.43	3.98	3.83	4.16	6.08	5.28	4.97	3.72
Y	8.14	4.14	5.54	6.29	10.84	8.66	7.75	14.29
Zr	4.03	1.468	2.71	2.505	12.42	6.01	3.35	8.34
Nb	0.0581					0.0118		
Cs								
Ba	0.97	0.191	0.064	0.103	0.096	0.152	0.252	0.336
La	0.125	0.066	0.11	0.0471	0.195	0.16	0.101	0.113
Ce	0.574	0.241	0.272	0.366	1.233	0.788	0.526	0.755
Pr	0.1185	0.054	0.0865	0.0861	0.318	0.1556	0.143	0.191
Nd	0.946	0.342	0.596	0.66	2.54	1.232	0.971	1.588
Sm	0.369	0.297	0.319	0.383	0.96	0.788	0.6	0.834
Eu	0.209	0.099	0.121	0.163	0.258	0.246	0.212	0.24
Gd	0.933	0.395	0.724	0.788	1.74	1.154	0.991	1.727
Tb	0.1813	0.085	0.1284	0.1543	0.311	0.236	0.175	0.326
Dy	1.339	0.784	1.005	1.181	2.09	1.709	1.323	2.8
Ho	0.294	0.157	0.228	0.264	0.448	0.354	0.31	0.597
Er	0.762	0.498	0.506	0.603	1.149	0.873	0.789	1.308
Tm	0.1328	0.0531	0.0883	0.1041	0.16	0.132	0.1056	0.243
Yb	0.977	0.566	0.618	0.729	1.4	0.926	0.904	1.622
Lu	0.1633	0.084	0.0841	0.096	0.21	0.1411	0.1115	0.228
Hf	0.179	0.08	0.096	0.113	0.468	0.29	0.201	0.292
Ta	0.0071				0.0047		0.0581	
Pb	0.123	0.152	0.127	0.106	0.028	0.054	0.088	0.618
Th					0.0092	0.0063	0.0095	0.0625
U	0.004				0.013	0.0113	0.0269	0.095

* calculated single clinopyroxene using the method of Putirka (2008); Mg#=Mg/(Mg+Fe)

Table S1(continued)

Sample	DJG13-65-2	DJG13-65-3	DJG13-65-4	DJG13-672-1	DJG13-672-2	DJG13-672-3	DJG13-65-5	DJG13-65-8
SiO_2	52.48	52.73	52.15	51.98	51.24	51.83	52.37	52.58
TiO_2	0.35	0.32	0.35	0.43	0.43	0.44	0.38	0.33
Al_2O_3	2.3	1.96	2.19	2.5	2.89	2.5	2.21	1.83
Cr_2O_3			0.03		0.04		0.06	
FeO	9.18	9.32	9.41	8.8	7.76	7.96	8.66	8.86
MnO	0.22	0.23	0.15	0.22	0.23	0.21	0.28	0.25
MgO	13.11	13.94	14.05	15.02	15.45	14.92	14.25	12.77
CaO	22.04	21.55	21.98	20.44	21.2	21.84	21.98	22.49
Na_2O	0.2	0.21	0.2	0.23	0.23	0.24	0.21	0.17
K_2O			0.02					
NiO	0.03					0.08	0.06	
Total	99.91	100.26	100.53	99.62	99.47	100.02	100.46	99.28
Si	1.9640	1.9612	1.9329	1.9336	1.9000	1.9176	1.9390	1.9829
Ti	0.0098	0.0089	0.0098	0.0120	0.0120	0.0122	0.0106	0.0094
Al	0.1014	0.0859	0.0957	0.1096	0.1263	0.1090	0.0964	0.0813
Cr	0.0000	0.0000	0.0009	0.0000	0.0012	0.0000	0.0018	0.0000
Fe^3	0.0000	0.0000	0.0335	0.0158	0.0652	0.0484	0.0177	0.0000
Fe^2	0.2873	0.2899	0.2582	0.2580	0.1754	0.1978	0.2504	0.2794
Fe	0.2873	0.2899	0.2916	0.2737	0.2406	0.2463	0.2681	0.2794
Mn	0.0070	0.0073	0.0047	0.0069	0.0072	0.0066	0.0088	0.0080
Mg	0.7314	0.7730	0.7763	0.8330	0.8541	0.8230	0.7866	0.7180
Ca	0.8836	0.8587	0.8728	0.8146	0.8422	0.8657	0.8719	0.9086
Na	0.0145	0.0151	0.0144	0.0166	0.0165	0.0172	0.0151	0.0124
K	0.0000	0.0000	0.0009	0.0000	0.0000	0.0000	0.0000	0.0000
Ni	0.0009	0.0000	0.0000	0.0000	0.0000	0.0024	0.0018	0.0000
Sum	4.0000	4.0000	4.0000	4.0000	4.0000	4.0000	4.0000	4.0000
Al(VI)	0.0753	0.0561	0.0383	0.0552	0.0382	0.0389	0.0460	0.0736
Al(IV)	0.0262	0.0298	0.0573	0.0544	0.0880	0.0701	0.0504	0.0077
En	38.31	40.08	39.91	43.20	43.93	42.39	40.64	37.51
Fs	15.41	15.40	15.23	14.56	12.75	13.02	14.31	15.02
Wo	46.28	44.52	44.86	42.25	43.32	44.59	45.05	47.47
Mg#	0.72	0.73	0.73	0.75	0.72	0.75	0.78	0.77
T(°C)*	1154	1164	1154	1182	1183	1176	1163	1137
Trace element (ppm)								
Li	1.033	0.477	0.255	0.476	0.486	0.841		
Be	0.049	0.043	0.146		0.042			
B	3.27	3.6	6.17	2.44	2.86	2.99		
P	34.87	36.97	96.64	36.29	39.85	37.18		
K	15	16.47	462.7	18.89	18.24	22.79		
Sc	190	169	308	132	133	139		
Ti	1973	2261	6676	2374	2352	2046		
V	604	552	1279	630	629	616		
Cr	10.51	11.03	19.51	206	179	183		
Mn	1839	1866	2404	1598	1670	1693		
Co	52	53.91	113.56	43.82	44.34	51.51		
Ni	82.38	78.25	302	165	164	180		
Cu	46.71	9.95	88.72	0.191	0.312	0.188		
Zn	50.87	51.88	142.23	32.46	34.1	41.55		
Ga	4.26	4.78	14.89	3.86	3.83	4.06		

Sample	DJG13-65-2	DJG13-65-3	DJG13-65-4	DJG13-672-1	DJG13-672-2	DJG13-672-3
Ge	2.44	2.81	4.87	1.85	2.28	2.16
As						
Rb		0.088				
Sr	2.9	3.59	12.27	3.77	3.88	3.27
Y	12.88	11	46.18	10.69	11.5	10.96
Zr	8.43	4.44	26.62	4.55	4.48	4.61
Nb			0.293			
Cs		0.028				
Ba		0.128	1.07	0.146	0.213	0.197
La	0.0945	0.1033	0.985	0.0697	0.097	0.0702
Ce	0.666	0.498	4.96	0.462	0.51	0.461
Pr	0.175	0.1345	0.967	0.1343	0.141	0.144
Nd	1.417	0.993	6.73	1.078	1.21	1.018
Sm	0.864	0.686	3.38	0.691	0.775	0.624
Eu	0.223	0.246	0.849	0.265	0.243	0.281
Gd	1.561	1.36	5.79	1.283	1.57	1.345
Tb	0.29	0.271	1.112	0.263	0.3	0.272
Dy	2.485	2.049	8.34	1.994	2.075	2.019
Ho	0.513	0.455	1.803	0.455	0.411	0.479
Er	1.216	1.021	4.02	1.011	0.977	1.085
Tm	0.223	0.1834	0.702	0.1806	0.2	0.184
Yb	1.492	1.252	4.61	1.229	1.181	1.17
Lu	0.2137	0.1758	0.64	0.1768	0.185	0.17
Hf	0.291	0.229	0.901	0.231	0.257	0.236
Ta			0.0135			0.0016
Pb	0.201		1.26			
Th	0.201		0.145		0.0029	
U	0.0456		0.0403	0.00149		

* calculated single clinopyroxene using the method of Putirka (2008); Mg#=Mg/(Mg+Fe)

Table S2 Major and Trace elements of the orthopyroxene from the gabbroic pegmatite and the plagiogranite in the Xigaze Ophiolite

Sample	DJG13-65-11	DJG13-65-12	DJG13-65-10	DJG13-67-2	DJG13-67-3	DJG13-67-4	DJG13-67-5
Lithology	Gabbroic pegmatite	Gabbroic pegmatite	Gabbroic pegmatite	Gabbroic pegmatite	Gabbroic pegmatite	Gabbroic pegmatite	Gabbroic pegmatite
SiO_2	54.12	53.74	53.48	53.59	54.46	54.21	54.47
TiO_2	0.29	0.16	0.22	0.18	0.19	0.09	0.09
Al_2O_3	1.8	1.09	1.47	1.04	2.19	1.29	1.26
Cr_2O_3		0.04			0.06		0.08
FeO	20.87	20.7	21.08	20.27	17.87	19.63	19.16
MnO	0.4	0.44	0.39	0.38	0.35	0.39	0.39
MgO	19.37	22.32	21.71	22.13	22.12	22.72	22.96
CaO	1.88	1.3	1.57	1.08	1.74	1.45	1.36
Na_2O	0.22	0.08	0.17		0.28		
K_2O						0.02	
NiO	0.07			0.06	0.08		0.04
Total	99.02	99.87	100.09	98.73	99.34	99.8	99.81
Si	2.0200	1.9890	1.9800	2.0010	1.9990	1.9950	2.0000
Ti	0.0080	0.0040	0.0060	0.0050	0.0050	0.0020	0.0020
Al	0.0790	0.0480	0.0640	0.0460	0.0950	0.0560	0.0550
Cr	0.0000	0.0010	0.0000	0.0000	0.0020	0.0000	0.0020
Fe^3	0.0000	0.0000	0.0000	0.0000	0.0000	0.0000	0.0000
Fe^2	0.6510	0.6410	0.6530	0.6330	0.5480	0.6040	0.5880
Mn	0.0130	0.0140	0.0120	0.0120	0.0110	0.0120	0.0120
Mg	1.0780	1.2310	1.1980	1.2310	1.2100	1.2460	1.2560
Ca	0.0750	0.0520	0.0620	0.0430	0.0680	0.0570	0.0540
Na	0.0160	0.0060	0.0120	0.0000	0.0200	0.0000	0.0000
K	0.0000	0.0000	0.0000	0.0000	0.0000	0.0010	0.0000
Sum	3.94	3.99	3.99	3.97	3.96	3.97	3.97
Mg#	0.62	0.66	0.65	0.66	0.69	0.67	0.68
Wo	4.16	2.70	3.24	2.25	3.72	2.99	2.85
En	59.76	63.98	62.62	64.55	66.27	65.34	66.17
Fs	36.09	33.32	34.13	33.19	30.01	31.67	30.98
Trace element (ppm)							
Li	0.0386	0.113					
Be	b.d.l	0.0049					
B	1.727	1.76					
P	21.6	24.38					
K	72.18	23.8					
Sc	46.75	22.6					
Ti	778	714					
V	206	150					
Cr	4.17	2.51					
Mn	1488	1590					
Co	59.77	66.39					
Ni	68.51	100.95					
Cu	0.287	0.924					
Zn	98.03	107.75					
Ga	2.524	2.586					
Ge	1.553	1.47					
Rb	b.d.l	b.d.l					
Sr	0.826	0.868					
Y	2.502	0.785					

Sample	DJG13-65-11	DJG13-65-12
Zr	3.12	2.591
Nb	0.0142	0.013
Cs	b.d.l	b.d.l
Ba	0.061	0.054
La	0.1177	0.0215
Ce	0.631	0.0935
Pr	0.1021	0.015
Nd	0.406	0.1
Sm	0.135	0.0173
Eu	0.0645	0.0173
Gd	0.176	0.031
Tb	0.0453	0.0068
Dy	0.357	0.1069
Ho	0.0971	0.0239
Er	0.267	0.0977
Tm	0.0586	0.0264
Yb	0.561	0.246
Lu	0.0947	0.0475
Hf	0.1106	0.0927
Ta	0.00147	0.00148
Pb	0.0267	b.d.l
Th	0.0257	0.0042
U	0.0081	0.0293

Mg#=Mg/(Mg+Fe); b.d.l, below detection limits

Table DR2 (Continued)

Sample	DJG13-67-6	DJG13-52-8	DJG13-54-1	DJG13-54-2	DJG13-54-3	DJG13-54-4
Lithology	Gabbroic pegmatite	Plagiogranite	Plagiogranite	Plagiogranite	Plagiogranite	Plagiogranite
SiO_2	54.27	55.71	53.71	53.71	53.42	53.72
TiO_2	0.1	0.19	0.14	0.13	0.2	0.06
Al_2O_3	1.31	0.93	1.2	0.92	1.03	0.68
Cr_2O_3						
FeO	19.06	20.47	20.73	20.72	20.59	20.99
MnO	0.37	0.55	0.59	0.61	0.52	0.6
MgO	23.31	20.8	21.37	21.39	21.62	21.63
CaO	1.18	1.01	1.93	1.69	1.53	1.26
Na_2O	0.02	0.22	0.19	0.17	0.18	0.15
K_2O		0.03				
NiO						
Total	99.62	99.91	99.86	99.34	99.09	99.09
Si	1.9940	2.0810	2.0010	2.0120	2.0030	2.0170
Ti	0.0030	0.0050	0.0040	0.0040	0.0060	0.0020
Al	0.0570	0.0410	0.0530	0.0410	0.0450	0.0300
Cr	0.0000					
Fe^3	0.0000	0.0000	0.0000	0.0000	0.0000	0.0000
Fe^2	0.5860	0.6390	0.6460	0.6490	0.6460	0.6590
Mn	0.0120	0.0170	0.0190	0.0190	0.0170	0.0190
Mg	1.2770	1.1580	1.1870	1.1940	1.2090	1.2110
Ca	0.0460	0.0400	0.0770	0.0680	0.0610	0.0510
Na	0.0010	0.0160	0.0140	0.0120	0.0130	0.0110
K	0.0000	0.0010	0.0000	0.0000	0.0000	0.0000
Sum	3.98	4.00	4.00	4.00	4.00	4.00
Mg#	0.69	0.64	0.65	0.65	0.65	0.65
Wo	2.41	2.18	4.00	3.51	3.18	2.61
En	66.89	62.42	61.55	61.87	62.55	62.42
Fs	30.70	35.40	34.46	34.62	34.27	34.97

Table S3 Major and Trace elements of the amphibole from the gabbroic pegmatite and the plagiogranite in the Xigaze Ophiolite.

Sample	DJG13-45-6	DJG13-45-7	DJG13-65-13	DJG13-492-1	DJG13-492-2	DJG13-492-3	DJG13-492-6
Lithology	Gabbroic pegmatite	Gabbroic pegmatite	Gabbroic pegmatite	Gabbroic pegmatite	Gabbroic pegmatite	Gabbroic pegmatite	Gabbroic pegmatite
SiO_2	51.7	50.4	49.96	51.03	51.28	52.7	46.91
TiO_2	0.79	1.17	1.13	0.54	0.81	0.71	1.92
Al_2O_3	5.37	6.53	6.09	5.01	4.51	3.53	8.45
Cr_2O_3	0.09	0.09	0.07	0.05		0.1	0.05
FeO	10.43	10.53	13.8	11.98	11.96	12.35	13.75
MnO	0.11	0.14	0.18	0.18	0.21	0.19	0.29
MgO	15.8	15.55	14.64	15.85	16.31	16.53	13.57
CaO	11.72	11.56	10.74	11.59	11.45	11.42	11.22
Na_2O	0.86	0.99	0.89	0.82	0.82	0.66	1.7
K_2O	0.09	0.03	0.03	0.08	0.09	0.1	0.07
NiO	0.09		0.07	0.08	0.05	0.06	
Total	97.05	96.99	97.6	97.21	97.49	98.35	97.93
Si(T)	7.3747	7.1879	7.0892	7.2705	7.2668	7.3943	6.7515
Al(IV)(T)	0.6253	0.8121	0.9108	0.7295	0.7332	0.5837	1.2485
Ti(T)	0.0000		0.0000	0.0000	0.0000	0.0220	0.0000
Al(VI)(C)	0.2774	0.2855	0.1076	0.1117	0.0199	0.0000	0.1847
Ti(C)	0.0848	0.1255	0.1206	0.0579	0.0863	0.0529	0.2078
Cr (C)	0.0101	0.0101	0.0079	0.0056	0.0000	0.0111	0.0057
Fe^{3+} (C)	0.3319	0.4537	1.0386	0.7172	0.8226	0.8361	0.6953
Mg (C)	3.3600	3.3062	3.0970	3.3666	3.4456	3.4577	2.9116
Fe^{2+} (C)	0.9121	0.8020	0.5988	0.7101	0.5946	0.6129	0.9595
Mn (C)	0.0133	0.0169	0.0216	0.0217	0.0252	0.0226	0.0353
Ca(C)	0.0103	0.0000	0.0080	0.0092	0.0057	0.0068	0.0000
Mg(B)	0.0000	0.0000	0.0000	0.0000	0.0000	0.0000	0.0000
Fe^{2+}(B)	0.0000	0.0000	0.0000	0.0000	0.0000	0.0000	0.0000
Mn(B)	0.0000	0.0000	0.0000	0.0000	0.0000	0.0000	0.0000
Ca(B)	1.7807	1.7663	1.6247	1.7599	1.7326	1.7098	1.7300
Na (B)	0.2193	0.2337	0.3753	0.2401	0.2674	0.2902	0.2700
Na (A)	0.0185	0.0400	-0.1305	-0.0136	-0.0421	-0.1106	0.2043
K (A)	0.0164	0.0055	0.0054	0.0145	0.0163	0.0179	0.0129
K(A)+Na(A)	0.0349	0.0454	-0.1251	0.0009	-0.0259	-0.0927	0.2172
(Ca+Na)(B)	2.0000	2.0000	2.0000	2.0000	2.0000	2.0000	2.0000
Na(B)	0.2193	0.2337	0.3753	0.2401	0.2674	0.2902	0.2700
Mg#	0.7865	0.8048	0.8380	0.8258	0.8528	0.8494	0.7521
T (°C)*	737	769	769	736	736	724	784
Uncertanty	56	56	22	22	22	22	22
Li	0.094	0.533					0.071
Be	0.149	0.053		0.124	0.073	0.251	0.193
B	5.65	6.09	2.62	2.25	2.29	2.46	3.8
P	78.58	77.17	56.74	59.56	53.95	50.33	93.38
K	757	358	483	522	356	610	391
Sc	97.28	96.52	95.52	77.46	86.95	48	125.58
Ti	6613	6526	4819	2250	2373	5005	9836
V	597	618	957	246	323	669	707
Cr	415	382	16	135	359	117	322
Mn	1280	1553	1550	1678	1792	1471	1914
Co	61.02	64.54	105.53	69.02	73.11	74.16	60.37
Ni	318.21	374.9	185.54	294.2	357.42	444.9	261.58
Cu	0.382	15.54	<0.214	0.174	0.247	0.252	
Zn	84.86	84.83	100.22	99.25	70.68	83.73	121.42

Sample	DJG13-45-6	DJG13-45-7	DJG13-65-13	DJG13-492-1	DJG13-492-2	DJG13-492-3	DJG13-492-6
Ga	9.17	9.03	9.25	7.44	5.98	9.05	12.53
Ge	2.31	2.23	2.66	2.36	2.3	2.4	2.72
As		0.26		0.391			
Rb	0.397	0.117	0.121	0.183	0.839	0.323	
Sr	11.27	10.98	4.55	3.49	3.39	4.14	15.58
Y	26.02	25.29	19.58	21.83	15.73	28.96	73.94
Zr	28.27	26.1	30.29	32.74	16.05	26.23	35.78
Nb	0.496	0.484	0.158	0.576	0.334	1.086	0.821
Cs					0.061		
Ba	1.14	0.59	0.77	0.514	0.97	1.2	1.27
La	0.958	0.792	0.851	1.391	1.246	2.511	1.133
Ce	4.81	4.41	4.22	5.86	4.76	9.47	6.16
Pr	1.003	1.061	0.843	1.013	0.745	1.594	1.591
Nd	6.55	6.48	4.83	5.35	3.72	9.01	12.24
Sm	2.34	2.29	1.591	1.867	1.161	3.19	6.18
Eu	0.77	0.709	0.515	0.625	0.468	0.779	1.593
Gd	3.31	3.2	2.02	2.67	1.584	4.4	9.88
Tb	0.584	0.609	0.362	0.468	0.313	0.742	1.771
Dy	4.42	4.4	3.04	3.56	2.56	5.37	13.29
Ho	0.951	0.894	0.666	0.774	0.57	1.164	2.884
Er	2.301	2.43	1.862	2	1.612	2.79	6.97
Tm	0.437	0.403	0.357	0.394	0.296	0.472	1.156
Yb	3.14	3.21	2.75	2.96	2.501	3.36	7.89
Lu	0.461	0.442	0.426	0.441	0.391	0.51	1.026
Hf	1.115	1.017	1.251	1.287	0.547	1.066	1.598
Ta	0.0247	0.0257	0.0147	0.0402	0.0264	0.0422	0.0317
Pb	0.058	0.079	0.041	0.031		0.044	0.059
Th	0.021	0.0062	0.0385	0.0388	0.0813	0.032	0.0153
U	0.0119	0.0108	0.0216	0.0235	0.033	0.0195	0.013

*calculated based on the method of Ridolfi et al. (2010)

Table S3 (Continued)

Sample	DJG13-492-5	DJG13-45-8	DJG13-45-11	DJG13-45-12	DJG13-45-13	DJG13-47-3	DJG13-47-4
Lithology	Gabbroic pegmatite	Gabbroic pegmatite	Gabbroic pegmatite	Gabbroic pegmatite	Gabbroic pegmatite	Gabbroic pegmatite	Gabbroic pegmatite
SiO_2	48.3	51.79	50.08	52.12	49.98	50.88	51.81
TiO_2	1.05	0.73	1.45	1	1.35	1	0.87
Al_2O_3	6.54	5.63	6.92	4.86	6.68	5.51	4.41
Cr_2O_3	0.1	0.07	0.08	0.1	0.09		0.04
FeO	13.57	10.3	11.12	9.94	10.68	13.93	13.61
MnO	0.28	0.22	0.18	0.13	0.19	0.16	0.26
MgO	14.65	15.95	15.04	16.26	15.15	13.44	14.08
CaO	11.29	11.62	11.67	11.84	12.05	11.13	11.33
Na_2O	1.19	0.87	1.18	0.75	1	0.87	0.84
K_2O	0.07	0.07	0.08	0.09	0.13	0.09	0.09
NiO	0.08	0.06	0.06	0.11	0.14	0.12	0.04
Total	97.12	97.31	97.86	97.2	97.44	97.13	97.38
Si(T)	6.9485	7.3457	7.1300	7.4107	7.1613	7.3459	7.4574
Al(IV)(T)	1.0515	0.6543	0.8700	0.5893	0.8387	0.6541	0.5426
Ti(T)	0.0000	0.0000	0.0000	0.0000	0.0000	0.0000	0.0000
Al(VI)(C)	0.0573	0.2868	0.2911	0.2251	0.2893	0.2834	0.2055
Ti(C)	0.1136	0.0779	0.1553	0.1069	0.1455	0.1086	0.0942
Cr (C)	0.0114	0.0078	0.0090	0.0112	0.0102	0.0000	0.0046
Fe^{3+} (C)	0.9309	0.4207	0.3592	0.3089	0.2472	0.4504	0.3990
Mg (C)	3.1420	3.3727	3.1923	3.4467	3.2362	2.8928	3.0214
Fe^{2+} (C)	0.7015	0.8009	0.9646	0.8729	1.0324	1.2313	1.2391
Mn (C)	0.0341	0.0264	0.0217	0.0157	0.0231	0.0196	0.0317
Ca(C)	0.0093	0.0068	0.0069	0.0126	0.0161	0.0139	0.0046
Mg(B)	0.0000	0.0000	0.0000	0.0000	0.0000	0.0000	0.0000
Fe^{2+}(B)	0.0000	0.0000	0.0000	0.0000	0.0000	0.0000	0.0000
Mn(B)	0.0000	0.0000	0.0000	0.0000	0.0000	0.0000	0.0000
Ca(B)	1.7308	1.7588	1.7731	1.7910	1.8336	1.7076	1.7425
Na (B)	0.2692	0.2412	0.2269	0.2090	0.1664	0.2924	0.2575
Na (A)	0.0627	-0.0019	0.0988	-0.0023	0.1114	-0.0489	-0.0231
K (A)	0.0128	0.0127	0.0145	0.0163	0.0238	0.0166	0.0165
K(A)+Na(A)	0.0755	0.0107	0.1133	0.0140	0.1351	-0.0323	-0.0066
(Ca+Na)(B)	2.0000	2.0000	2.0000	2.0000	2.0000	2.0000	2.0000
Na(B)	0.2692	0.2412	0.2269	0.2090	0.1664	0.2924	0.2575
Mg#	0.8175	0.8081	0.7679	0.7979	0.7581	0.7014	0.7092
T (°C)*	763	741	782	731	782	725	703
Uncertanty	22	56	56	56	56	56	56

Table S3 (Continued)

Sample	DJG13-47-12	DJG13-47-13	DJG13-49-1	DJG13-49-2	DJG13-49-3	DJG13-49-5	DJG13-49-6
Lithology	Gabbroic pegmatite	Gabbroic pegmatite	Gabbroic pegmatite	Gabbroic pegmatite	Gabbroic pegmatite	Gabbroic pegmatite	Gabbroic pegmatite
SiO2	50.35	49.98	49.72	50.44	49.66	52.2	50.89
TiO2	0.58	0.57	0.49	0.39	0.41	0.46	0.74
Al2O3	6.74	7.23	7.29	6.08	6.7	4.96	6.15
Cr2O3	0.03		0.04	0.07	0.05	0.04	0.03
FeO	12.15	12.41	10.51	11.77	12.71	8.67	9.54
MnO	0.18	0.14	0.22	0.11	0.14	0.16	0.16
MgO	14.62	13.96	16.85	16.4	15.8	19.01	18.14
CaO	11.12	11.26	11.59	11.76	11.5	11.72	11.62
Na2O	1.1	1.29	1.22	0.85	1.02	0.82	0.96
K2O	0.07	0.06	0.12	0.1	0.11	0.07	0.1
NiO	0.08		0.07			0.11	
Total	97.02	96.9	98.12	97.97	98.1	98.22	98.33
Si(T)	7.1988	7.2004	6.9604	7.1013	7.0016	7.2010	7.0474
Al(IV)(T)	0.8012	0.7996	1.0396	0.8987	0.9984	0.7990	0.9526
Ti(T)	0.0000	0.0000	0.0000	0.0000	0.0000	0.0000	0.0000
Al(VI)(C)	0.3344	0.4279	0.1631	0.1100	0.1148	0.0073	0.0511
Ti(C)	0.0624	0.0618	0.0516	0.0413	0.0435	0.0477	0.0771
Cr (C)	0.0034	0.0000	0.0044	0.0078	0.0056	0.0044	0.0033
Fe^{3+} (C)	0.6144	0.4011	0.9399	0.9009	1.0185	0.9961	1.0208
Mg (C)	3.1162	2.9983	3.5166	3.4421	3.3210	3.9096	3.7451
Fe^{2+} (C)	0.8381	1.0939	0.2904	0.4847	0.4800	0.0040	0.0840
Mn (C)	0.0218	0.0171	0.0261	0.0131	0.0167	0.0187	0.0188
Ca(C)	0.0092	0.0000	0.0079	0.0000	0.0000	0.0122	0.0000
Mg(B)	0.0000	0.0000	0.0000	0.0000	0.0000	0.0000	0.0000
Fe^{2+}(B)	0.0000	0.0000	0.0000	0.0000	0.0000	0.0000	0.0000
Mn(B)	0.0000	0.0000	0.0000	0.0000	0.0000	0.0000	0.0000
Ca(B)	1.6941	1.7379	1.7303	1.7737	1.7370	1.7199	1.7240
Na (B)	0.3059	0.2621	0.2697	0.2263	0.2630	0.2801	0.2760
Na (A)	-0.0010	0.0982	0.0615	0.0057	0.0158	-0.0608	-0.0183
K (A)	0.0128	0.0110	0.0214	0.0180	0.0198	0.0123	0.0177
K(A)+Na(A)	0.0117	0.1092	0.0829	0.0237	0.0356	-0.0485	-0.0006
(Ca+Na)(B)	2.0000	2.0000	2.0000	2.0000	2.0000	2.0000	2.0000
Na(B)	0.3059	0.2621	0.2697	0.2263	0.2630	0.2801	0.2760
Mg#	0.7881	0.7327	0.9237	0.8766	0.8737	0.9990	0.9781
T (°C)*	755	764	800	766	777	763	784
Uncertanty	56	56	22	22	22	22	22

Table S3 (Continued)

Sample	DJG13-49-9	DJG13-49-10	DJG13-49-11	DJG13-65-14	DJG13-67-1	DJG13-492-4	DJG13-48-4
Lithology	Gabbroic pegmatite	Gabbroic pegmatite	Gabbroic pegmatite	Gabbroic pegmatite	Gabbroic pegmatite	Gabbroic pegmatite	Gabbroic pegmatite
SiO2	50.46	49.83	50.35	49.87	49.19	49.55	46.53
TiO2	0.44	0.76	0.59	0.68	1.6	1.06	2.32
Al2O3	5.83	6.22	7.3	5.64	7.89	5.84	9.17
Cr2O3			0.11		0.03	0.04	0.11
FeO	13.06	13.22	8.87	16.49	11.37	13	13.59
MnO	0.18	0.24	0.15	0.22	0.09	0.22	0.17
MgO	15.86	15.82	18.4	12.83	14.2	14.86	12.49
CaO	11.25	11.02	11.01	10.99	10.98	11.57	11.01
Na2O	0.92	0.97	1.23	0.73	1.62	0.94	2.06
K2O	0.07	0.06	0.15	0.14		0.1	0.04
NiO			0.04		0.09		0.07
Total	98.07	98.14	98.2	97.59	97.06	97.18	97.56
Si(T)	7.1010	6.9975	6.9271	7.1930	7.0628	7.1199	6.7697
Al(IV)(T)	0.8990	1.0025	1.0729	0.8070	0.9372	0.8801	1.2303
Ti(T)	0.0000	0.0000	0.0000	0.0000	0.0000	0.0000	0.0000
Al(VI)(C)	0.0678	0.0269	0.1107	0.1517	0.3978	0.1089	0.3419
Ti(c)	0.0466	0.0803	0.0611	0.0738	0.1728	0.1146	0.2539
Cr (C)	0.0000	0.0000	0.0120	0.0000	0.0034	0.0045	0.0127
Feiii (C)	1.0824	1.2244	1.2281	0.8814	0.3616	0.6952	0.3473
Mg (C)	3.3273	3.3120	3.5881	2.7588	3.0396	3.1833	2.7091
Feii (C)	0.4544	0.3279	0.0000	1.1074	1.0035	0.8668	1.3060
Mn (C)	0.0215	0.0285	0.0000	0.0269	0.0109	0.0268	0.0209
Ca(C)	0.0000	0.0000	0.0000	0.0000	0.0104	0.0000	0.0082
Mg(B)	0.0000	0.0000	0.1858	0.0000	0.0000	0.0000	0.0000
Feii(B)	0.0000	0.0000	0.0000	0.0000	0.0000	0.0000	0.0000
Mn(B)	0.0000	0.0000	0.0175	0.0000	0.0000	0.0000	0.0000
Ca(B)	1.6961	1.6579	1.6228	1.6982	1.6786	1.7811	1.7079
Na (B)	0.3039	0.3421	0.3772	0.3018	0.3214	0.2189	0.2921
Na (A)	-0.0529	-0.0780	-0.0491	-0.0977	0.1295	0.0429	0.2890
K (A)	0.0126	0.0107	0.0263	0.0258	0.0000	0.0183	0.0074
K(A)+Na(A)	-0.0404	-0.0673	-0.0228	-0.0719	0.1295	0.0613	0.2964
(Ca+Na)B	2.0000	2.0000	2.0000	2.0000	2.0000	2.0000	2.0000
NaB	0.3039	0.3421	0.3772	0.3018	0.3214	0.2189	0.2921
Mg#	0.8798	0.9099	1.0000	0.7136	0.7518	0.7860	0.6747
T (°C)*	761	779		740	793	761	840
Uncertanty	22	22		22	56	22	56

Table S3 (Continued)

Sample	DJG13-48-5	DJG13-48-6	DJG13-48-8	DJG13-48-9	DJG13-65-6	DJG13-65-9	DJG13-52-1
Lithology	Gabbroic pegmatite	Gabbroic pegmatite	Gabbroic pegmatite	Gabbroic pegmatite	Gabbroic pegmatite	Gabbroic pegmatite	Plagiogranite
SiO2	46.64	46.87	47.22	48.44	47.44	52.52	47.5
TiO2	2.4	2.3	2.25	1.33	0.68	0.23	0.09
Al2O3	9.15	8.95	8.87	8.07	7.03	3.44	7.04
Cr2O3	0.1	0.05	0.24	0.13	0.05	0.03	
FeO	13.22	12.83	13.17	12.81	18.76	11.45	23.11
MnO	0.18	0.14	0.15	0.2	0.19	0.2	0.24
MgO	13.35	13.25	13.15	14.11	10.75	17.7	6.79
CaO	11.01	11.06	10.83	11.07	11.3	11.81	11.86
Na2O	1.93	1.9	1.8	1.51	1	0.38	0.68
K2O	0.02	0.05	0.04	0.09	0.06	0.02	0.17
NiO			0.08				
Total	98	97.4	97.8	97.76	97.26	97.78	97.48
Si(T)	6.7058	6.7862	6.7932	6.9223	6.9970	7.3493	7.2210
Al(IV)(T)	1.2942	1.2138	1.2068	1.0777	1.0030	0.5673	0.7790
Ti(T)	0.0000	0.0000	0.0000	0.0000	0.0000	0.0242	0.0000
Al(VI)(C)	0.2562	0.3133	0.2971	0.2814	0.2180	0.0000	0.4820
Ti(c)	0.2595	0.2505	0.2435	0.1430	0.0750	0.0000	0.0100
Cr (C)	0.0114	0.0057	0.0273	0.0147	0.0060	0.0033	0.0000
Feiii (C)	0.5740	0.4202	0.5478	0.6714	0.7610	1.0349	0.1790
Mg (C)	2.8615	2.8600	2.8203	3.0061	2.3640	3.6925	1.5390
Feii (C)	1.0154	1.1331	1.0365	0.8593	1.5530	0.2694	2.7590
Mn (C)	0.0219	0.0172	0.0183	0.0242	0.0240	0.0000	0.0310
Ca(C)	0.0000	0.0000	0.0093	0.0000	0.0000	0.0000	0.0000
Mg(B)	0.0000	0.0000	0.0000	0.0000	0.0000	0.0000	0.0000
Feii(B)	0.0000	0.0000	0.0000	0.0000	0.0000	0.0355	0.0000
Mn(B)	0.0000	0.0000	0.0000	0.0000	0.0000	0.0237	0.0000
Ca(B)	1.6959	1.7156	1.6599	1.6948	1.7860	1.7705	1.9320
Na (B)	0.3041	0.2844	0.3401	0.3052	0.2140	0.2295	0.0680
Na (A)	0.2339	0.2489	0.1619	0.1131	0.0720	-0.1264	0.1320
K (A)	0.0037	0.0092	0.0073	0.0164	0.0110	0.0036	0.0330
K(A)+Na(A)	0.2376	0.2581	0.1693	0.1295	0.0830	-0.1229	0.1650
(Ca+Na)B	2.0000	2.0000	2.0000	2.0000	2.0000	2.0000	2.0000
NaB	0.3041	0.2844	0.3401	0.3052	0.2140	0.2295	0.0680
Mg#	0.7381	0.7162	0.7313	0.7777	0.6035	0.9320	0.3581
T (°C)*	846	838	828	803	757	753	
Uncertanty	22	22	22	22	22	22	

Table S3 (Continued)

Sample	DJG13-52-3	DJG13-52-4	DJG13-52-5	DJG13-52-7
Lithology	Plagiogranite	Plagiogranite	Plagiogranite	Plagiogranite
SiO2	47.54	49.25	50.62	50.72
TiO2	0.08	0.04	0.06	0.05
Al2O3	6.83	4.86	4.35	4.77
Cr2O3		0.03	0.04	
FeO	23.26	24.13	22.7	22.91
MnO	0.12	0.17	0.25	0.2
MgO	6.99	7.16	7.39	7.48
CaO	12.1	11.77	11.24	11.43
Na2O	0.79	0.39	0.28	0.24
K2O	0.28	0.12	0.03	0.04
NiO		0.04	0.04	
Total	97.99	97.96	97	97.84
Si(T)	7.2180	7.4430	7.6490	7.5920
Al(IV)(T)	0.7820	0.5570	0.3510	0.4080
Ti(T)	0.0000	0.0000	0.0000	0.0000
Al(VI)(C)	0.4400	0.3080	0.4230	0.4320
Ti(C)	0.0090	0.0050	0.0070	0.0060
Cr (C)	0.0000	0.0040	0.0050	0.0000
Fe^{3+} (C)	0.1000	0.2880	0.1820	0.2220
Mg (C)	1.5820	1.6130	1.6650	1.6690
Fe^{2+} (C)	2.8540	2.7610	2.6860	2.6460
Mn (C)	0.0150	0.0220	0.0320	0.0250
Ca(C)	0.0000	0.0000	0.0000	0.0000
Mg(B)	0.0000	0.0000	0.0000	0.0000
Fe^{2+}(B)	0.0000	0.0000	0.0000	0.0000
Mn(B)	0.0000	0.0000	0.0000	0.0000
Ca(B)	1.9680	1.9060	1.8200	1.8330
Na (B)	0.0320	0.0940	0.0820	0.0700
Na (A)	0.2010	0.0200	0.0000	0.0000
K (A)	0.0540	0.0230	0.0060	0.0080
K(A)+Na(A)	0.2550	0.0430	0.0060	0.0080
(Ca+Na)(B)	2.0000	2.0000	1.9020	1.9030
Na(B)	0.0320	0.0940	0.0820	0.0700
Mg#	0.3566	0.3688	0.3827	0.3868

Table S4 Whole rock analyses of clinopyroxene megacryst, gabbroic pegmatite, plagiogranite, basaltic and diabase dike/enclave, pillow basalt

Sample No.	DJG13-45	DJG13-48	DJG13-49	DJG13-66	DJ12-16
Lithology	Clinopyroxene megacryst	Clinopyroxene megacryst	Gabbroic pegmatite	Gabbroic pegmatite	Plagiogranite
SiO_2	48.26	49.20	50.48	49.92	55.40
TiO_2	0.26	0.82	0.41	0.77	0.51
Al_2O_3	5.86	4.67	13.15	15.16	16.89
TFe_2O_3	7.17	9.49	7.64	8.06	10.92
MnO	0.18	0.24	0.13	0.15	0.19
MgO	15.85	14.40	9.98	8.41	3.38
CaO	18.23	18.99	11.80	9.78	7.05
Na_2O	0.26	0.42	2.27	2.99	3.37
K_2O	0.05	0.06	0.80	1.10	0.26
P_2O_5	0.01	0.01	0.03	0.06	0.04
LOI	3.86	1.47	2.47	3.07	1.72
Total	100.00	99.76	99.15	99.47	99.73
Li	3.05	3.14	2.24	2.75	1.95
Cu	30.35	24.41	8.03	8.90	79.99
Zn	54.02	74.42	51.10	66.20	93.04
Ga	6.52	7.97	13.28	7.78	16.54
Cs	b.d.l	b.d.l	b.d.l	b.d.l	0.05
Rb	b.d.l	b.d.l	4.37	b.d.l	1.48
Ba	1.28	1.22	14.90	2.60	15.88
Th	0.12	0.10	0.15	0.10	0.09
U	0.06	0.07	0.09	0.07	0.03
Ta	0.02	0.06	0.05	0.02	0.06
Nb	0.10	0.38	0.57	0.24	0.72
La	b.d.l	0.13	1.24	b.d.l	0.31
Ce	0.57	2.83	5.75	0.70	1.32
Pb	0.22	0.15	0.31	0.21	0.86
Pr	0.25	0.70	0.95	0.25	0.26
Sr	13	13	158	5	112.44
Nd	1.72	5.03	5.50	1.60	1.61
Zr	9.36	21.22	20.18	6.29	21.54
Hf	0.42	0.90	0.79	0.30	0.69
Sm	0.78	2.41	1.99	0.62	0.76
Eu	0.28	0.69	0.58	0.32	0.37
Gd	1.12	3.38	2.54	0.80	1.26
Tb	0.26	0.77	0.55	0.18	0.31
Dy	1.90	5.52	3.88	1.30	2.25
Y	12.25	27.08	24.99	8.82	14.29
Ho	0.41	1.15	0.82	0.28	0.54
Er	1.19	3.29	2.43	0.87	1.66
Tm	0.18	0.48	0.36	0.13	0.28
Yb	1.15	3.03	2.43	0.91	1.93
Lu	0.18	0.45	0.38	0.15	0.31
V	612.40	818.46	342.59	235.33	340.24
Sc	71.89	106.10	41.29	28.81	47.53
Co	76.82	75.79	58.62	63.62	30.20
Cr	357.00	224.48	131.16	70.64	15.93
Ni	150.95	102.42	81.91	69.21	18.54

Table S4 (Continued)

Sample No.	DJ12-18	DJ12-17	DJ12-15	DJ12-19	DJ12-21
Lithology	Plagiogranite	Plagiogranite	Plagiogranite	Plagiogranite	Plagiogranite
SiO_2	59.30	61.92	77.38	75.40	75.99
TiO_2	0.59	0.38	0.12	0.22	0.22
Al_2O_3	15.75	16.44	12.32	12.36	12.13
TFe_2O_3	9.06	7.80	1.46	2.85	2.62
MnO	0.16	0.15	0.02	0.06	0.05
MgO	2.90	2.04	0.31	0.60	0.43
CaO	6.77	5.87	1.80	2.99	3.15
Na_2O	3.61	3.52	5.37	4.38	4.18
K_2O	0.28	0.30	0.12	0.14	0.13
P_2O_5	0.05	0.06	0.03	0.06	0.06
LOI	1.47	1.51	0.99	0.90	0.61
Total	99.93	99.97	99.93	99.95	99.57
Li	4.36	3.58	0.09	0.13	0.12
Cu	19.83	17.67	41.05	1.30	0.70
Zn	73.90	76.40	11.05	32.66	27.20
Ga	15.90	15.31	10.89	13.31	13.31
Cs	0.05	0.05	0.04	0.03	0.03
Rb	1.54	1.00	0.21	0.15	0.21
Ba	16.08	16.21	19.57	10.21	11.40
Th	0.15	0.13	0.18	0.15	0.14
U	0.04	0.05	0.22	0.09	0.08
Ta	0.08	0.09	0.19	0.09	0.09
Nb	0.87	0.94	1.20	1.01	1.01
La	0.84	1.22	2.45	1.18	1.12
Ce	2.52	3.45	7.70	4.31	3.93
Pb	0.87	1.04	1.07	1.26	1.15
Pr	0.45	0.65	1.09	0.60	0.60
Sr	111.85	97.48	89.23	69.27	64.77
Nd	2.42	3.71	5.36	3.14	3.27
Zr	39.46	31.01	105.21	139.56	111.33
Hf	1.12	1.13	3.95	3.65	2.94
Sm	0.97	1.36	1.84	1.04	1.18
Eu	0.39	0.44	0.32	0.52	0.57
Gd	1.56	2.00	2.61	1.47	1.81
Tb	0.36	0.43	0.61	0.31	0.38
Dy	2.56	3.15	4.54	2.27	2.88
Y	15.95	20.68	29.87	16.00	19.87
Ho	0.61	0.75	1.11	0.55	0.71
Er	1.85	2.30	3.47	1.79	2.22
Tm	0.30	0.38	0.57	0.31	0.37
Yb	2.09	2.59	3.97	2.29	2.56
Lu	0.34	0.42	0.66	0.40	0.43
V	334.48	224.84	19.73	15.95	10.40
Sc	37.92	31.22	4.82	3.66	4.91
Co	25.52	20.76	3.91	3.92	3.70
Cr	14.82	17.83	7.74	5.51	5.27
Ni	26.00	18.77	38.81	0.69	0.31

Table S4 (Continued)

Sample No.	DJ12-22	DJG13-96	DJG13-52	DJG13-53	DJG13-54
Lithology	Plagiogranite	Plagiogranite	Plagiogranite	Plagiogranite	Plagiogranite
SiO_2	75.06	68.87	71.10	66.95	61.53
TiO_2	0.19	0.43	0.25	0.53	0.54
Al_2O_3	12.42	13.43	15.18	17.84	18.33
TFe_2O_3	2.45	3.14	1.71	2.79	3.85
MnO	0.05	0.05	0.03	0.04	0.07
MgO	0.55	2.94	0.93	1.35	2.38
CaO	2.35	1.25	2.51	2.44	4.86
Na_2O	5.11	6.80	6.22	6.67	5.57
K_2O	0.12	0.33	0.62	1.15	1.05
P_2O_5	0.05	0.10	0.04	0.13	0.09
LOI	1.19	2.48	1.00	0.10	1.23
Total	99.53	99.82	99.61	99.99	99.51
Li	2.15	3.71	b.d.l	b.d.l	b.d.l
Cu	2.86	5.72	2.43	5.31	4.19
Zn	26.53	23.15	9.14	15.05	32.07
Ga	13.40	13.81	14.61	17.35	17.27
Cs	0.02	0.31	b.d.l	b.d.l	b.d.l
Rb	0.90	0.00	1.35	4.22	3.96
Ba	13.35	22.20	16.72	20.72	13.02
Th	0.26	0.11	0.12	0.14	0.14
U	0.12	0.09	0.10	0.10	0.11
Ta	0.11	0.04	0.07	0.10	0.11
Nb	1.25	0.29	0.64	1.47	1.35
La	2.86	0.26	1.47	3.20	2.07
Ce	7.24	1.47	4.13	9.52	7.95
Pb	0.95	0.17	0.61	0.67	0.60
Pr	1.19	0.27	0.58	1.36	1.37
Sr	70.27	166.27	115	158	196
Nd	6.11	1.38	2.84	7.09	8.20
Zr	98.09	20.63	124.93	113.51	69.67
Hf	2.93	0.61	3.61	3.50	2.51
Sm	2.01	0.46	0.70	1.87	3.03
Eu	0.60	0.21	0.80	0.85	1.04
Gd	2.93	0.71	0.83	2.15	3.92
Tb	0.64	0.16	0.16	0.39	0.86
Dy	4.88	1.21	1.08	2.49	6.04
Y	31.24	8.47	7.53	15.84	31.18
Ho	1.17	0.28	0.25	0.52	1.30
Er	3.63	0.90	0.84	1.59	3.91
Tm	0.59	0.14	0.14	0.24	0.59
Yb	4.02	1.01	1.06	1.67	3.87
Lu	0.65	0.17	0.19	0.29	0.59
V	12.14	44.40	24.25	30.51	56.89
Sc	8.47	13.97	2.74	3.89	9.64
Co	3.07	11.07	4.92	7.87	18.35
Cr	6.03	0.00	0.32	0.00	2.14
Ni	1.89	11.98	6.40	6.22	16.70

Table S4 (Continued)

Sample No.	DJ12-08	DJ12-09	DJ12-14	DJ12-20	DJG13-75
Lithology	Basaltic dike	Diabase	Diabase pocket	Diabase enclave	Pillow basalt
SiO_2	49.88	49.94	52.13	52.89	49.78
TiO_2	0.56	0.44	0.26	0.21	0.97
Al_2O_3	14.05	13.73	12.51	10.86	14.90
TFe_2O_3	9.67	8.05	9.47	9.41	8.54
MnO	0.16	0.14	0.15	0.17	0.13
MgO	11.09	11.32	11.01	12.61	6.49
CaO	7.43	9.80	8.28	9.15	8.06
Na_2O	3.76	3.01	2.95	2.31	5.25
K_2O	0.004	0.19	0.11	0.17	0.12
P_2O_5	0.06	0.05	0.03	0.02	0.10
LOI	3.17	2.75	2.35	2.14	5.57
Total	99.84	99.43	99.24	99.95	99.91
Li	2.42	2.88	1.70	2.46	9.63
Cu	62.65	37.15	199.76	42.77	77.06
Zn	71.41	44.75	49.78	57.94	83.12
Ga	12.74	10.73	9.80	9.48	13.95
Cs	0.01	0.08	0.03	0.04	0.001
Rb	1.62	2.84	2.58	2.13	0.00
Ba	2.63	4.29	6.92	9.39	6.96
Th	0.07	0.03	0.02	0.35	0.14
U	0.04	0.02	0.02	0.06	0.25
Ta	0.04	0.02	0.01	0.02	0.08
Nb	0.44	0.25	0.12	0.18	0.95
La	1.21	0.84	0.56	0.91	2.58
Ce	3.63	2.71	1.44	2.15	9.92
Pb	0.21	0.42	0.48	0.33	0.44
Pr	0.64	0.50	0.22	0.31	1.53
Sr	61.46	142.65	111.77	70.49	96
Nd	3.56	2.94	1.10	1.50	8.48
Zr	40.52	28.77	16.42	26.46	85.01
Hf	1.11	0.82	0.47	0.62	2.59
Sm	1.28	1.09	0.46	0.50	2.74
Eu	0.44	0.43	0.19	0.21	0.92
Gd	1.78	1.54	0.77	0.78	3.22
Tb	0.39	0.33	0.18	0.17	0.66
Dy	2.74	2.28	1.37	1.28	4.38
Y	15.80	12.91	8.75	8.22	26.52
Ho	0.61	0.50	0.33	0.30	0.91
Er	1.78	1.44	1.01	0.91	2.67
Tm	0.27	0.22	0.16	0.14	0.39
Yb	1.78	1.42	1.11	0.96	2.54
Lu	0.28	0.22	0.19	0.16	0.40
V	205.51	189.16	220.10	192.22	224.90
Sc	36.45	40.42	44.64	42.92	25.87
Co	35.23	34.35	39.22	44.57	46.51
Cr	327.01	552.42	548.51	740.68	108.18
Ni	144.22	153.20	174.11	266.33	49.67

Table S4 (Continued)

Sample No.	DJG13-81	DJG13-83	DJG13-89	DJG13-98	DJG13-100	DJG13-68
Lithology	Pillow basalt	Pillow basalt	Pillow basalt	Pillow basalt	Pillow basalt	Pillow basalt
SiO_2	46.62	49.19	51.92	50.58	52.89	51.92
TiO_2	0.75	1.18	1.05	1.09	1.02	0.73
Al_2O_3	13.69	15.47	15.11	14.10	15.29	14.41
TFe_2O_3	7.02	9.64	8.87	9.46	9.36	7.32
MnO	0.13	0.18	0.14	0.12	0.17	0.10
MgO	7.48	6.18	5.59	4.11	5.70	7.45
CaO	13.11	5.85	8.82	10.60	6.40	8.93
Na_2O	3.21	4.93	5.31	4.38	4.29	3.52
K_2O	0.11	0.24	0.13	0.24	1.20	0.08
P_2O_5	0.09	0.09	0.09	0.15	0.11	0.07
LOI	7.62	7.20	2.90	4.83	2.79	5.48
Total	99.81	100.16	99.94	99.67	99.22	100.00
Li	12.15	4.06	3.31	24.86	28.55	13.00
Cu	57.48	81.59	36.57	37.58	38.15	74.61
Zn	69.82	88.05	77.90	94.32	104.23	74.27
Ga	14.18	17.44	14.68	14.45	17.35	13.54
Cs	0.001	0.001	0.001	0.001	0.334	0.001
Rb	0.00	0.22	0.00	1.07	24.64	0.00
Ba	3.81	6.66	8.77	12.81	22.57	4.29
Th	0.12	0.15	0.14	0.20	0.17	0.13
U	0.11	0.09	0.11	0.11	0.15	0.19
Ta	0.05	0.09	0.08	0.10	0.09	0.12
Nb	0.63	1.09	1.07	1.28	1.23	0.99
La	1.75	2.78	2.22	4.20	3.00	1.79
Ce	7.02	10.51	8.74	13.75	10.78	7.09
Pb	0.58	0.72	0.40	0.70	0.79	0.38
Pr	1.12	1.60	1.36	1.95	1.60	1.13
Sr	92	125	119	155	207	82
Nd	6.33	8.95	7.72	10.69	8.94	6.31
Zr	59.82	86.72	71.41	97.34	81.79	58.54
Hf	1.82	2.65	2.26	2.92	2.57	1.85
Sm	2.10	2.94	2.54	3.30	2.93	2.07
Eu	0.74	1.13	0.92	1.12	1.02	0.74
Gd	2.53	3.55	3.04	3.90	3.58	2.51
Tb	0.52	0.73	0.62	0.78	0.73	0.51
Dy	3.52	4.91	4.14	5.18	4.99	3.45
Y	24.13	26.14	26.78	28.11	28.96	23.41
Ho	0.73	1.02	0.86	1.06	1.03	0.71
Er	2.14	2.96	2.54	3.10	3.04	2.12
Tm	0.31	0.43	0.37	0.45	0.44	0.31
Yb	2.08	2.79	2.41	2.96	2.90	2.05
Lu	0.32	0.43	0.37	0.45	0.45	0.32
V	285.72	241.42	227.04	188.84	242.83	278.68
Sc	24.22	26.84	26.00	26.71	30.15	24.11
Co	45.19	46.87	42.80	44.82	50.35	49.28
Cr	133.23	22.11	45.63	86.94	77.24	122.15
Ni	55.94	16.36	23.30	43.41	30.86	58.00

Table S4 (Continued)

Sample No.	DJG13-71	DJG13-73	DJG13-79	DJG13-91	DJG13-93	DJG13-95
Lithology	Pillow basalt	Pillow basalt	Pillow basalt	Pillow basalt	Pillow basalt	Pillow basalt
SiO_2	55.90	50.30	55.28	53.39	50.31	51.89
TiO_2	0.79	0.84	0.90	0.78	0.77	0.57
Al_2O_3	13.44	14.37	13.41	14.71	15.27	16.53
TFe_2O_3	7.17	7.61	6.43	8.25	8.64	7.08
MnO	0.11	0.13	0.11	0.15	0.15	0.12
MgO	6.99	6.55	4.99	6.34	8.47	7.98
CaO	7.39	9.24	9.30	7.89	9.91	7.34
Na_2O	4.17	4.33	4.10	5.40	2.98	4.51
K_2O	0.09	0.09	0.09	0.13	1.11	0.39
P_2O_5	0.09	0.09	0.10	0.07	0.06	0.05
LOI	3.68	5.96	5.20	2.28	1.99	3.16
Total	99.81	99.54	99.90	99.39	99.66	99.62
Li	11.75	8.97	5.88	3.31	10.59	13.24
Cu	61.10	66.97	71.25	19.52	97.66	47.72
Zn	70.04	72.24	89.97	76.15	76.37	47.47
Ga	14.00	14.66	13.01	13.98	15.42	13.85
Cs	0.001	0.001	0.001	0.001	0.001	0.001
Rb	0.00	0.00	0.00	0.00	12.73	4.27
Ba	3.52	4.71	3.52	8.88	14.78	7.93
Th	0.13	0.13	0.13	0.13	0.12	0.12
U	0.12	0.22	0.41	0.12	0.10	0.09
Ta	0.06	0.07	0.07	0.06	0.05	0.04
Nb	0.74	0.86	0.87	0.73	0.62	0.47
La	1.84	2.19	2.13	1.63	1.42	1.02
Ce	7.52	8.52	8.32	6.69	6.25	4.86
Pb	0.35	0.57	0.35	0.56	0.39	0.35
Pr	1.21	1.32	1.29	1.07	1.03	0.81
Sr	56	59	59	126	136	220
Nd	6.84	7.47	7.29	6.20	5.95	4.65
Zr	63.95	73.88	73.58	67.17	64.89	56.86
Hf	1.99	2.26	2.28	1.88	1.71	1.49
Sm	2.22	2.38	2.31	2.13	2.03	1.59
Eu	0.75	0.80	0.81	0.79	0.76	0.61
Gd	2.61	2.86	2.73	2.64	2.48	1.97
Tb	0.53	0.58	0.55	0.55	0.52	0.40
Dy	3.51	3.83	3.65	3.74	3.50	2.74
Y	23.17	26.75	24.06	24.91	23.31	18.07
Ho	0.72	0.81	0.76	0.78	0.72	0.57
Er	2.11	2.36	2.22	2.27	2.12	1.69
Tm	0.30	0.35	0.32	0.34	0.31	0.25
Yb	1.96	2.25	2.10	2.17	2.01	1.64
Lu	0.31	0.35	0.33	0.33	0.31	0.26
V	205.29	179.26	196.47	207.26	220.09	175.97
Sc	22.66	25.56	25.42	27.90	30.21	26.81
Co	38.69	41.86	44.44	49.11	53.36	47.03
Cr	97.67	97.11	107.37	67.16	109.80	82.46
Ni	36.27	35.92	51.78	29.85	41.49	40.15

Table S5 Whole-rock Sr-Nd isotopes of gabbroic pegmatite and plagiogranite in the Xigaze Ophiolite

Sample No.	DJ12-16	DJ12-19	DJ12-22	DJG13-96	DJG13-52	DJG13-53	DJG13-54	DJG13-45	DJG13-48	DJG13-49	DJG13-66
Lithology	Plagio-granite	Plagio-granite	Plagio-granite	Plagio-granite	Plagio-granite	Plagio-granite	Plagio-granite	Clinopyroxene megacryst	Clinopyroxene megacryst	Gabbroic pegmatite	Gabbroic pegmatite
T (Ma)	125	125	125	125	125	125	125	125	125	125	125
Rb (ppm)	1.48	0.15	0.9		1.35	4.22	3.96			4.37	
Sr (ppm)	112.44	69.27	70.27	166	115	158	196	13	13	158	5
$^{87}Rb/^{87}Sr$	0.038065	0.006262	0.037038	0.000000	0.033945	0.077233	0.058423			0.079979	
$^{87}Sr/^{86}Sr$	0.704505	0.703729	0.704029	0.703756	0.703465	0.703522	0.703482	0.703779	0.703783	0.703603	0.706044
2σ	0.00001	0.000008	0.000005	0.000005	0.000005	0.000011	0.000004	0.000009	0.000004	0.000007	0.000007
$(^{87}Sr/^{86}Sr)i$	0.704437	0.703717	0.703963	0.703756	0.703405	0.703385	0.703378	0.703779	0.703783	0.703461	0.706044
Sm (ppm)	0.76	1.04	2.01	0.46	0.7	1.87	3.03	0.78	2.41	1.99	0.62
Nd (ppm)	1.61	3.14	6.11	1.38	2.84	7.09	8.2	1.72	5.03	5.5	1.6
$^{147}Sm/^{144}Nd$	0.285416	0.200255	0.198899	0.201542	0.149025	0.159477	0.223419	0.274210	0.289696	0.218766	0.234310
$^{143}Nd/^{144}Nd$	0.513135	0.51304	0.513006	0.513107	0.513019	0.51327	0.513143	0.513402	0.513171	0.513123	0.51341
2σ	0.00001	0.000003	0.000005	0.000015	0.00001	0.000012	0.000006	0.000015	0.000005	0.000007	0.000007
$(^{143}Nd/^{144}Nd)i$	0.512902	0.512876	0.512843	0.512942	0.512897	0.513140	0.512960	0.513178	0.512934	0.512944	0.513218
$\varepsilon_{Nd}(t)$	8.3	7.8	7.1	9.1	8.2	12.9	9.4	13.7	8.9	9.1	14.5
T_{DM}(Ma)	-32	1258	1493	546	310	-340	-109	634	42	-797	1905
$f_{Sm/Nd}$	0.4510201	0.0180748	0.0111774	0.0246171	-0.242376	-0.189235	0.135835	0.394053	0.472782	0.112179	0.191202

Errors shown in table are within-run statistics and represent error in the last significant digits. The following is the external reproducibility at 2σ: Nd = +30 ppm; Sr = +30 ppm. Sr and Nd isotope compositions are normalized to $^{86}Sr/^{88}Sr = 0.1194$ and $^{146}Nd/^{144}Nd = 0.7219$, respectively. Rb, Sr, Sm, and Nd concentrations (in ppm) are analyzed by inductively coupled plasma–mass spectrometry.

Table S6 LA-ICP-MS U-Pb data for zircon from plagiogranite in the Xigaze Ophiolite

				CORRECTED RATIOS					
Analysis No.	Th (ppm)	U (ppm)	Th/U	$^{207}Pb/^{206}Pb$	1σ	$^{207}Pb/^{235}U$	1σ	$^{206}Pb/^{238}U$	1σ
DJ12-17-01	60	109	0.55	0.04833	0.00227	0.12354	0.00559	0.01854	0.00038
DJ12-17-02	16	59	0.28	0.0516	0.00438	0.1366	0.01112	0.0192	0.00056
DJ12-17-03	26	94	0.28	0.04868	0.00304	0.12679	0.00759	0.01889	0.00045
DJ12-17-04	22	77	0.29	0.04874	0.00325	0.13255	0.0085	0.01972	0.00048
DJ12-17-05	60	129	0.46	0.04907	0.00226	0.13082	0.00574	0.01933	0.00041
DJ12-17-06	34	139	0.25	0.04816	0.00244	0.14084	0.00677	0.02121	0.00049
DJ12-17-07	31	105	0.30	0.04826	0.00332	0.12585	0.00822	0.01891	0.00051
DJ12-17-08	18	69	0.26	0.04847	0.00325	0.1271	0.0082	0.01902	0.00046
DJ12-17-09	20	93	0.21	0.04844	0.00276	0.12481	0.00681	0.01869	0.00043
DJ12-17-10	14	48	0.30	0.0484	0.00453	0.12903	0.0117	0.01933	0.00055
DJ12-17-11	37	118	0.32	0.04875	0.00271	0.12775	0.00675	0.01901	0.00045
DJ12-17-12	76	214	0.36	0.04859	0.00182	0.12204	0.00435	0.01822	0.00036
DJ12-17-13	40	101	0.40	0.04876	0.0028	0.12718	0.00699	0.01892	0.00044
DJ12-17-14	41	100	0.41	0.0491	0.00286	0.12875	0.00719	0.01902	0.00044
DJ12-17-15	64	195	0.33	0.05249	0.00268	0.13929	0.00667	0.01925	0.00047
DJ12-17-16	68	150	0.45	0.04952	0.00252	0.11894	0.00574	0.01742	0.0004
DJ12-17-17	41	95	0.43	0.04845	0.00295	0.12879	0.00749	0.01928	0.00046
DJ12-17-18	10	41	0.25	0.05142	0.00735	0.14308	0.01963	0.02018	0.00089
DJ12-17-19	29	81	0.36	0.04836	0.003	0.12168	0.00732	0.01825	0.00041
DJ12-17-20	32	73	0.44	0.04873	0.00396	0.1356	0.01054	0.02018	0.00058
DJ12-19-01	36	82	0.44	0.04951	0.00363	0.13295	0.00946	0.01948	0.00047
DJ12-19-02	30	82	0.36	0.04841	0.00305	0.12786	0.00777	0.01916	0.00044
DJ12-19-03	14	37	0.38	0.04881	0.00682	0.13221	0.0179	0.01965	0.00075
DJ12-19-04	22	69	0.31	0.04936	0.00523	0.12387	0.01261	0.0182	0.00061
DJ12-19-05	2	9	0.23	0.05318	0.03504	0.15022	0.09752	0.02049	0.00236
DJ12-19-06	65	105	0.62	0.04927	0.00307	0.12778	0.0077	0.01881	0.00043
DJ12-19-07	15	38	0.39	0.04892	0.00846	0.14585	0.02441	0.02163	0.00102
DJ12-19-08	12	27	0.44	0.04859	0.0081	0.1295	0.02109	0.01933	0.00075
DJ12-19-09	37	69	0.53	0.04857	0.00521	0.12495	0.01283	0.01866	0.00065
DJ12-19-10	10	27	0.36	0.04841	0.00917	0.12866	0.02374	0.01928	0.00089
DJ12-19-11	12	28	0.42	0.04883	0.00835	0.13173	0.02198	0.01957	0.00081
DJ12-19-12	69	124	0.56	0.04865	0.00299	0.12266	0.00718	0.01829	0.00046
DJ12-19-13	38	72	0.53	0.04847	0.00459	0.13177	0.01188	0.01972	0.00065
DJ12-19-14	22	42	0.51	0.04936	0.00714	0.1413	0.01966	0.02077	0.0009

Table S6 (Continued)

Analysis No.	Th (ppm)	U (ppm)	Th/U	CORRECTED RATIOS $^{207}Pb/^{206}Pb$	1σ	$^{207}Pb/^{235}U$	1σ	$^{206}Pb/^{238}U$	1σ
DJG13-96-001	36	133	0.27	0.0496	0.01176	0.12469	0.02945	0.01823	0.00048
DJG13-96-002	25	67	0.37	0.04771	0.02736	0.13233	0.07562	0.02011	0.00104
DJG13-96-003	190	209	0.91	0.04884	0.01078	0.13099	0.02879	0.01945	0.00051
DJG13-96-004	58	157	0.37	0.04812	0.01387	0.13519	0.03876	0.02037	0.00069
DJG13-96-005	500	511	0.98	0.0489	0.00403	0.13198	0.01085	0.01957	0.00035
DJG13-96-006	46	63	0.73	0.04811	0.03546	0.13438	0.09869	0.02025	0.00128
DJG13-96-007	39	92	0.42	0.04875	0.02401	0.13958	0.06848	0.02076	0.00095
DJG13-96-008	115	178	0.64	0.04846	0.00887	0.12978	0.02367	0.01942	0.00043
DJG13-96-009	30	82	0.37	0.05043	0.02353	0.13113	0.06093	0.01886	0.00085
DJG13-96-010	33	101	0.33	0.04944	0.01902	0.14379	0.05505	0.02109	0.00087
DJG13-96-011	26	64	0.41	0.04793	0.03387	0.12233	0.08616	0.01851	0.0011
DJG13-96-012	38	85	0.45	0.05054	0.01816	0.14353	0.05137	0.02059	0.00073
DJG13-96-013	33	42	0.78	0.04961	0.04325	0.14469	0.12578	0.02116	0.00143
DJG13-96-014	153	149	1.03	0.04767	0.01321	0.12483	0.0345	0.019	0.00051
DJG13-96-015	241	305	0.79	0.04844	0.00562	0.13479	0.01558	0.02019	0.0004
DJG13-96-016	47	53	0.89	0.04908	0.04384	0.12829	0.11425	0.01896	0.00138
DJG13-96-017	41	49	0.83	0.04849	0.04126	0.11709	0.09934	0.01752	0.00119
DJG13-96-018	22	50	0.44	0.04937	0.0354	0.15091	0.10781	0.02218	0.00141
DJG13-96-019	19	31	0.59	0.04891	0.05533	0.1215	0.1371	0.01802	0.00151
DJG13-96-020	40	102	0.40	0.05042	0.02356	0.14374	0.06689	0.02068	0.00097
DJG13-96-021	78	138	0.57	0.0481	0.01288	0.12884	0.03436	0.01944	0.00056
DJG13-96-022	390	215	1.82	0.04869	0.01102	0.13663	0.03076	0.02036	0.00058
DJG13-96-023	91	235	0.39	0.04841	0.01115	0.13046	0.02985	0.01955	0.00061
DJG13-52-001**	9.9	23.3	0.43	0.05123	0.163	0.07904	0.25069	0.01119	0.00285
DJG13-52-002	23.9	39.9	0.60	0.05185	0.05278	0.13887	0.14081	0.01943	0.00181
DJG13-52-003	57.7	46.0	1.26	0.04937	0.03222	0.14373	0.09346	0.02112	0.00121
DJG13-52-004	16.9	28.2	0.60	0.04972	0.06184	0.13021	0.16144	0.019	0.00194
DJG13-52-005*	6.4	14.2	0.45	0.05257	0.09158	0.20331	0.35311	0.02806	0.00384
DJG13-52-006**	90.6	75.0	1.21	0.04837	0.03215	0.11103	0.07351	0.01665	0.00102
DJG13-52-007	7.8	17.8	0.44	0.04862	0.11777	0.13318	0.32164	0.01987	0.00371
DJG13-52-008	17.5	24.6	0.71	0.05136	0.07402	0.15604	0.22416	0.02204	0.00258
DJG13-52-009	25.8	37.3	0.69	0.04926	0.04315	0.13037	0.11384	0.0192	0.00138
DJG13-52-010*	17.4	30.5	0.57	0.05318	0.027	0.31516	0.15942	0.04299	0.00201
DJG13-52-011	18.7	37.2	0.50	0.04882	0.04984	0.13338	0.13577	0.01982	0.00161
DJG13-52-012	15.7	30.5	0.51	0.0517	0.05192	0.14087	0.14099	0.01977	0.00168
DJG13-52-013	25.1	35.0	0.72	0.04904	0.03917	0.14024	0.11166	0.02074	0.00135
DJG13-52-014**	12.2	21.6	0.56	0.04794	0.14704	0.08124	0.24857	0.01229	0.00269
DJG13-52-015	18.6	32.0	0.58	0.05091	0.07505	0.1228	0.18047	0.0175	0.00205
DJG13-52-016**	44.3	40.7	1.09	0.0492	0.06234	0.09006	0.11377	0.01328	0.00134
DJG13-52-017	36.4	37.5	0.97	0.04912	0.03743	0.1324	0.10058	0.01955	0.00122
DJG13-52-018	23.4	30.0	0.78	0.05132	0.0437	0.14636	0.12425	0.02069	0.00145
DJG13-52-019	93.1	72.7	1.28	0.04946	0.02737	0.12715	0.07015	0.01865	0.00087
DJG13-52-020	13.5	23.6	0.57	0.05129	0.06412	0.12968	0.16163	0.01834	0.00182
DJG13-52-021	12.5	25.3	0.49	0.05443	0.0671	0.12973	0.15936	0.01729	0.00181
DJG13-52-022	17.3	27.4	0.63	0.0532	0.04993	0.1394	0.13037	0.01901	0.00151

Table S6 (Continued)

	CORRECTED RATIOS				CORRECTED AGES (Ma)							
	$^{208}Pb/^{232}Th$	1σ	$^{238}U/^{232}Th$	1σ	$^{207}Pb/^{206}Pb$	1σ	$^{207}Pb/^{235}U$	1σ	$^{206}Pb/^{238}U$	1σ	$^{208}Pb/^{232}Th$	1σ
DJ12-17-01	0.00496	0.0004	4.53	0.02	115	107	118	5	118	2	100	8
DJ12-17-02	0.00734	0.00141	9.05	0.05	268	194	130	10	123	4	148	28
DJ12-17-03	0.00613	0.00092	9	0.04	132	141	121	7	121	3	124	18
DJ12-17-04	0.00633	0.00103	8.75	0.04	135	151	126	8	126	3	128	21
DJ12-17-05	0.00542	0.00048	5.42	0.02	151	106	125	5	123	3	109	10
DJ12-17-06	0.00677	0.00091	10.15	0.04	107	114	134	6	135	3	136	18
DJ12-17-07	0.00503	0.00094	8.41	0.04	112	154	120	7	121	3	101	19
DJ12-17-08	0.00513	0.00106	9.51	0.05	122	151	121	7	121	3	103	21
DJ12-17-09	0.0054	0.00103	11.79	0.05	121	129	119	6	119	3	109	21
DJ12-17-10	0.00675	0.00135	8.31	0.05	119	208	123	11	123	3	136	27
DJ12-17-11	0.00609	0.00077	8.03	0.03	136	126	122	6	121	3	123	15
DJ12-17-12	0.00568	0.00045	7.12	0.02	128	87	117	4	116	2	114	9
DJ12-17-13	0.00629	0.00067	6.38	0.03	136	130	122	6	121	3	127	13
DJ12-17-14	0.00606	0.00066	6.13	0.03	153	133	123	6	121	3	122	13
DJ12-17-15	0.00744	0.00077	7.67	0.03	307	119	132	6	123	3	150	15
DJ12-17-16	0.00675	0.00055	5.62	0.02	173	118	114	5	111	3	136	11
DJ12-17-17	0.00608	0.00066	5.84	0.03	121	137	123	7	123	3	123	13
DJ12-17-18	0.007	0.0027	10.04	0.07	260	303	136	17	129	6	141	54
DJ12-17-19	0.00531	0.00076	7.12	0.04	117	140	117	7	117	3	107	15
DJ12-17-20	0.00483	0.00089	5.8	0.03	135	183	129	9	129	4	97	18
DJ12-19-01	0.00548	0.00074	4.91	0.29	172	167	127	8	124	3	110	15
DJ12-19-02	0.00575	0.00074	5.97	0.35	119	142	122	7	122	3	116	15
DJ12-19-03	0.00614	0.00167	5.61	0.33	139	280	126	16	125	5	124	34
DJ12-19-04	0.00541	0.00142	6.94	0.41	165	238	119	11	116	4	109	29
DJ12-19-05	0.01413	0.01521	9.49	0.58	336	1060	142	86	131	15	284	303
DJ12-19-06	0.00529	0.00052	3.5	0.21	161	142	122	7	120	3	107	10
DJ12-19-07	0.00815	0.00225	5.53	0.33	144	321	138	22	138	6	164	45
DJ12-19-08	0.00856	0.00182	4.9	0.29	128	311	124	19	123	5	172	36
DJ12-19-09	0.00454	0.00092	4.05	0.24	127	237	120	12	119	4	92	19
DJ12-19-10	0.00536	0.00236	6.02	0.36	119	342	123	21	123	6	108	47
DJ12-19-11	0.00551	0.0018	5.1	0.3	140	317	126	20	125	5	111	36
DJ12-19-12	0.00471	0.00048	3.82	0.23	131	139	117	6	117	3	95	10
DJ12-19-13	0.00632	0.00087	4.02	0.24	122	211	126	11	126	4	127	17
DJ12-19-14	0.0036	0.00126	4.14	0.25	165	290	134	17	133	6	73	25

Table S6 (Continued)

	CORRECTED RATIOS				CORRECTED AGES (Ma)							
	$^{208}Pb/^{232}Th$	1σ	$^{238}U/^{232}Th$	1σ	$^{207}Pb/^{206}Pb$	1σ	$^{207}Pb/^{235}U$	1σ	$^{206}Pb/^{238}U$	1σ	$^{208}Pb/^{232}Th$	1σ
DJG13-96-001	0.00311	0.00213	7.67	0.04	176	418	119	27	116	3	63	43
DJG13-96-002	0.00192	0.00397	5.66	0.04	85	968	126	68	128	7	39	80
DJG13-96-003	0.00544	0.00104	2.3	0.01	140	391	125	26	124	3	110	21
DJG13-96-004	0.00119	0.00204	5.64	0.02	105	482	129	35	130	4	24	41
DJG13-96-005	0.00542	0.00084	2.14	0.01	143	186	126	10	125	2	109	17
DJG13-96-006	0.00706	0.00287	2.87	0.02	105	1113	128	88	129	8	142	58
DJG13-96-007	0.00584	0.00321	4.96	0.03	136	845	133	61	132	6	118	65
DJG13-96-008	0.00528	0.00106	3.25	0.01	122	336	124	21	124	3	106	21
DJG13-96-009	0.00458	0.00321	5.62	0.03	215	829	125	55	120	5	92	65
DJG13-96-010	-0.00041	0.00311	6.32	0.03	169	657	136	49	135	5	-8	63
DJG13-96-011	-0.00188	0.00405	5.1	0.03	96	1055	117	78	118	7	-38	82
DJG13-96-012	0.00744	0.00247	4.64	0.03	220	625	136	46	131	5	150	50
DJG13-96-013	0.00734	0.00417	3.17	0.03	177	1163	137	112	135	9	148	84
DJG13-96-014	0.00499	0.00127	2.41	0.01	83	460	119	31	121	3	101	26
DJG13-96-015	0.0065	0.00132	3.14	0.01	121	245	128	14	129	3	131	27
DJG13-96-016	0.00401	0.00335	2.79	0.02	152	1173	123	103	121	9	81	67
DJG13-96-017	0.00065	0.00297	2.98	0.02	123	1135	112	90	112	8	13	60
DJG13-96-018	-0.00334	0.00605	5.66	0.04	165	1093	143	95	141	9	-68	123
DJG13-96-019	0.00193	0.00562	4.2	0.04	144	1351	116	124	115	10	39	113
DJG13-96-020	0.00892	0.00457	6.22	0.03	214	831	136	59	132	6	179	92
DJG13-96-021	0.00826	0.00216	4.38	0.02	104	450	123	31	124	4	166	43
DJG13-96-022	0.00649	0.00131	1.36	0.01	133	396	130	27	130	4	131	26
DJG13-96-023	0.00705	0.00231	6.38	0.02	119	401	125	27	125	4	142	46
DJG13-52-001*	0.02126	0.01734	4.97	0.3	251	3551	77	236	72	18	425	343
DJG13-52-002	0.00371	0.00668	3.54	0.21	279	1289	132	126	124	11	75	135
DJG13-52-003	0.00901	0.0027	1.69	0.1	165	1028	136	83	135	8	181	54
DJG13-52-004	0.01583	0.00824	3.53	0.21	182	1465	124	145	121	12	317	164
DJG13-52-005*	0.00031	0.02158	4.67	0.28	310	2006	188	298	178	24	6	436
DJG13-52-006*	0.00384	0.00188	1.75	0.1	117	1020	107	67	106	6	77	38
DJG13-52-007	-0.0255	0.02047	4.83	0.29	130	2801	127	288	127	23	-522	425
DJG13-52-008	0.016	0.00934	2.97	0.18	257	1584	147	197	141	16	321	186
DJG13-52-009	-0.00131	0.00473	3.06	0.18	160	1165	124	102	123	9	-26	96
DJG13-52-010*	0.02469	0.00901	3.72	0.22	336	925	278	123	271	12	493	178
DJG13-52-011	-0.00169	0.00749	4.21	0.25	139	1266	127	122	127	10	-34	152
DJG13-52-012	0.00627	0.00773	4.13	0.25	272	1282	134	125	126	11	126	155
DJG13-52-013	0.00233	0.00443	2.95	0.18	150	1112	133	99	132	9	47	89
DJG13-52-014*	0.01486	0.01265	3.76	0.23	96	3486	79	233	79	17	298	252
DJG13-52-015	-0.00244	0.00884	3.64	0.22	237	1607	118	163	112	13	-49	179
DJG13-52-016*	0.00249	0.00292	1.94	0.12	157	1461	88	106	85	9	50	59
DJG13-52-017	0.00814	0.00324	2.18	0.13	154	1139	126	90	125	8	164	65
DJG13-52-018	0.00579	0.00462	2.72	0.16	255	1170	139	110	132	9	117	93
DJG13-52-019	0.00741	0.00199	1.65	0.1	170	964	122	63	119	6	149	40
DJG13-52-020	0.00802	0.00793	3.69	0.22	254	1491	124	145	117	12	161	159
DJG13-52-021	0.00662	0.00936	4.29	0.26	389	1528	124	143	111	11	133	188
DJG13-52-022	-0.00105	0.00586	3.35	0.2	337	1285	133	116	121	10	-21	119

*Inherited zircon ages that are excluded from weighted mean age calculation;

**Abnormal ages that are younger than other analyses;

GPS location: 29°06′8.08″N,89°05′8.37″E (sample DJG13-52); 29°09′01″N, 89°06′12″E (sample DJG12-17 and DJG12-19); 29°09′3.56″N, 89°11′58.21″E (sample DJG13-96).

Table S7 LA-ICP-MS Lu-Hf data for zircon from plagiogranite in the Xigaze Ophiolite

Analysis No.	Ages	1σ	$^{176}Yb/^{177}Hf$	2σ	$^{176}Lu/^{177}Hf$	2σ	$^{176}Hf/^{177}Hf$	2σ	$\varepsilon_{Hf}(0)$	$\varepsilon_{Hf}(t)$	T_{DM} (Ma)	T_{DM}^{C} (Ma)
DJ12-17-01	118	2	0.129381	0.0006	0.005351	0.000019	0.283072	0.000021	10.6	12.8	287	338
DJ12-17-02	123	4	0.121799	0.0009	0.004909	0.000035	0.283097	0.000022	11.5	13.8	245	283
DJ12-17-03	121	3	0.111413	0.0019	0.004678	0.000051	0.283126	0.000025	12.5	14.8	197	222
DJ12-17-04	126	3	0.138472	0.0017	0.005563	0.000047	0.283129	0.000025	12.6	14.9	198	218
DJ12-17-05	123	3	0.179322	0.0031	0.007004	0.000102	0.283155	0.000026	13.6	15.7	161	170
DJ12-17-06	135	3	0.144782	0.005	0.005899	0.000191	0.283164	0.000023	13.9	16.3	141	142
DJ12-17-07	121	3	0.132089	0.0009	0.005685	0.000018	0.283104	0.000027	11.7	13.9	239	273
DJ12-17-08	121	3	0.137443	0.0048	0.005747	0.000163	0.283020	0.000027	8.8	11.0	377	449
DJ12-17-09	119	3	0.139747	0.0025	0.006031	0.000105	0.283161	0.000029	13.8	15.9	147	154
DJ12-17-10	123	3	0.110828	0.0025	0.004628	0.000090	0.283105	0.000023	11.8	14.1	229	264
DJ12-17-11	121	3	0.146012	0.0073	0.005913	0.000294	0.283105	0.000034	11.8	13.9	239	272
DJ12-17-12	116	2	0.135852	0.0016	0.005477	0.000066	0.283077	0.000033	10.8	12.9	281	329
DJ12-17-13	121	3	0.187675	0.0097	0.007527	0.000369	0.283078	0.000029	10.8	12.9	297	335
DJ12-17-14	121	3	0.087766	0.0045	0.003735	0.000186	0.283123	0.000028	12.4	14.8	195	222
DJ12-17-15	123	3	0.143056	0.0005	0.006147	0.000013	0.283134	0.000025	12.8	15.0	192	211
DJ12-17-16	111	3	0.158560	0.007	0.006560	0.000287	0.283065	0.000026	10.3	12.3	311	361
DJ12-17-17	123	3	0.188861	0.0023	0.007770	0.000088	0.283091	0.000025	11.3	13.4	277	308
DJ12-17-18	129	6	0.123607	0.0042	0.005268	0.000161	0.283140	0.000025	13.0	15.4	177	191
DJ12-17-19	117	3	0.097873	0.0019	0.004215	0.000085	0.283073	0.000024	10.6	12.9	277	332
DJ12-17-20	129	4	0.148470	0.0032	0.006080	0.000122	0.283093	0.000024	11.4	13.7	260	295
DJ12-19- 01	124	3	0.131993	0.0054	0.005109	0.000176	0.283075	0.000024	10.7	13.0	281	329
DJ12-19-02	122	3	0.184197	0.0023	0.006819	0.000067	0.283122	0.000022	12.4	14.5	216	239
DJ12-19-03	125	5	0.171582	0.0025	0.006426	0.000053	0.283174	0.000026	14.2	16.4	127	128
DJ12-19-04	116	4	0.148072	0.0019	0.005616	0.000065	0.283110	0.000022	12.0	14.1	228	260
DJ12-19-05	131	15	0.088010	0.0035	0.003372	0.000135	0.283056	0.000024	10.0	12.6	296	358
DJ12-19-06	120	3	0.152634	0.0028	0.005599	0.000092	0.283085	0.000025	11.1	13.3	268	311
DJ12-19-07	138	6	0.077903	0.0011	0.003015	0.000039	0.283113	0.000026	12.0	14.8	207	235
DJ12-19-08	123	5	0.090739	0.0009	0.003450	0.000021	0.283126	0.000027	12.5	14.9	190	215
DJ12-19-09	119	4	0.222293	0.0074	0.008133	0.000257	0.283087	0.000026	11.1	13.1	288	321
DJ12-19-10	123	6	0.069514	0.0021	0.002647	0.000078	0.283114	0.000030	12.1	14.6	203	235
DJ12-19-11	125	5	0.095978	0.001	0.003753	0.000038	0.283124	0.000031	12.5	14.9	194	219
DJ12-19-12	117	3	0.122504	0.0011	0.004472	0.000028	0.283146	0.000023	13.2	15.5	163	179
DJ12-19-13	126	4	0.129784	0.0011	0.004750	0.000038	0.283169	0.000024	14.0	16.4	129	130
DJ12-19-14	133	6	0.083570	0.001	0.003052	0.000035	0.283122	0.000028	12.4	15.0	193	217

$\varepsilon_{Hf(0)} = ((^{176}Hf/^{177}Hf)_S/(^{176}Hf/^{177}Hf)_{CHUR,0}-1)\times10000$

$\varepsilon_{Hf(t)} = ((^{176}Hf/^{177}Hf)_S-(^{176}Lu/^{177}Hf)_S\times(e^{lt}-1))/((^{176}Hf/^{177}Hf)_{CHUR,0}-(^{176}Lu/^{177}Hf)_{CHUR}\times(e^{lt}-1))-1)\times10000$

$T_{DM} = 1/\lambda\times(1+((^{176}Hf/^{177}Hf)_S-(^{176}Hf/^{177}Hf)_{DM})/((^{176}Lu/^{177}Hf)_S-(^{176}Lu/^{177}Hf)_{DM}))$

$T_{DM}^{C}=T_{DM}-(T_{DM}-t)*((f_{CC}-f_S)/(f_{CC}-f_{DM}))$

$f_{Lu/Hf} = (^{176}Lu/^{177}Hf)_S/(^{176}Lu/^{177}Hf)_{CHUR}-1$

where, $(^{176}Lu/^{177}Hf)_S$ and $(^{176}Hf/^{177}Hf)_S$ are the measured values of samples, $(^{176}Lu/^{177}Hf)_{CHUR} = 0.0332$ and $(^{176}Hf/^{177}Hf)_{CHUR,0} = 0.282772$ (Blichert-Toft and Albarède, 1997);

$(^{176}Lu/^{177}Hf)_{DM} = 0.0384$ and $(^{176}Hf/^{177}Hf)_{DM} = 0.28325$ (Griffin et al., 2000), $\lambda = 1.867\times10^{-11}$/y (Söderlund et al., 2004), $(^{176}Lu/^{177}Hf_{mean\ crust})=0.015$ (Griffin et al., 2002)

$f_{CC}=(^{176}Lu/^{177}Hf_{mean\ crust})/(^{176}Lu/^{177}Hf)_{CHUR}-1$; $f_{DM}=(^{176}Lu/^{177}Hf)_{DM}/(^{176}Lu/^{177}Hf)_{CHUR}-1$

References

Blichert-Toft, J., and Albarède, F., 1997, The Lu-Hf isotope geochemistry of chondrites and the evolution of the mantle-crust system: Earth and Planetary Science Letters, v. 148, no. 1, p. 243-258. doi: 10.1016/S0012-821X(97)00040-X

Griffin, W. L., Pearson, N. J., Belousova, E., Jackson, S. E., van Achterbergh, E., O'Reilly, S. Y., and Shee, S. R., 2000, The Hf isotope composition of cratonic mantle: LAM-MC-ICPMS analysis of zircon megacrysts in kimberlites: Geochimica et Cosmochimica Acta, v. 64, no. 1, p. 133-147. doi: 10.1016/S0016-7037(99)00343-9

Söderlund, U., Patchett, P. J., Vervoort, J. D., and Isachsen, C. E., 2004, The 176Lu decay constant determined by Lu–Hf and U–Pb isotope systematics of Precambrian mafic intrusions: Earth and Planetary Science Letters, v. 219, no. 3, p. 311-324. doi: 10.1016/S0012-821X(04)00012-3

Griffin, W. L., Wang, X., Jackson, S. E., Pearson, N. J., O'Reilly, S. Y., Xu, X., and Zhou, X., 2002, Zircon chemistry and magma mixing, SE China: In-situ analysis of Hf isotopes, Tonglu and Pingtan igneous complexes: Lithos, v. 61, no. 3, p. 237-269. doi: 10.1016/S0024-4937(02)00082-8

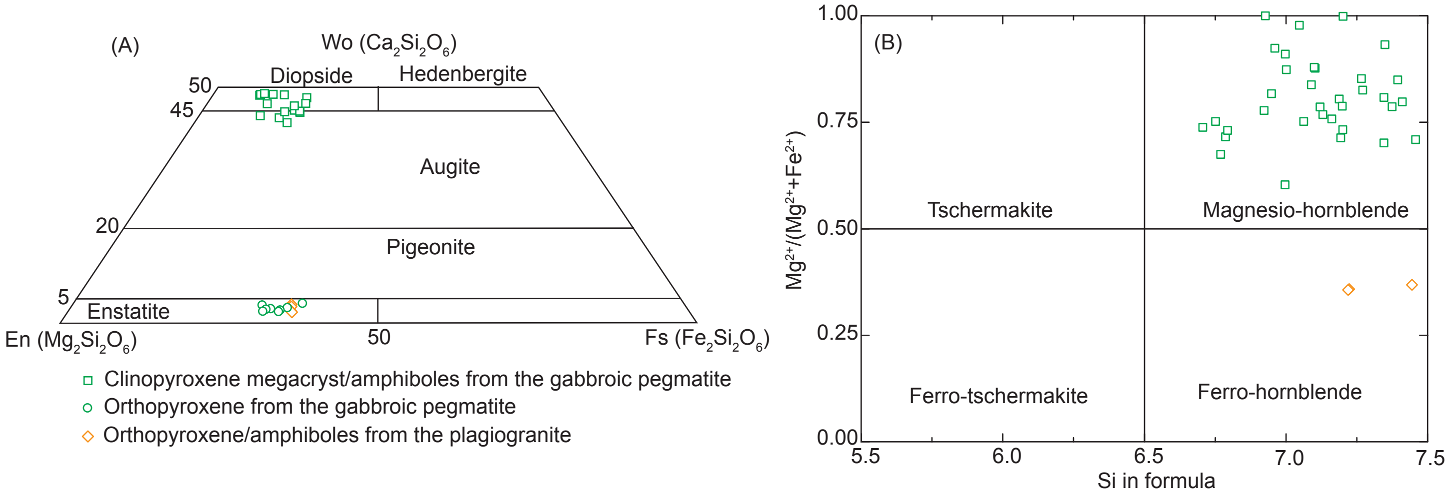
(A)
Wo ($Ca_2Si_2O_6$)
Diopside
Hedenbergite
50
45
Augite
20
Pigeonite
5
Enstatite
En ($Mg_2Si_2O_6$)
50
Fs ($Fe_2Si_2O_6$)
Clinopyroxene megacryst/amphiboles from the gabbroic pegmatite
Orthopyroxene from the gabbroic pegmatite
Orthopyroxene/amphiboles from the plagiogranite
(B)
1.00
0.75
0.50
0.25
0.00
$Mg^{2+}/(Mg^{2+}+Fe^{2+})$
Tschermakite
Magnesio-hornblende
Ferro-tschermakite
Ferro-hornblende
5.5
6.0
6.5
7.0
7.5
Si in formula

Figure DR2

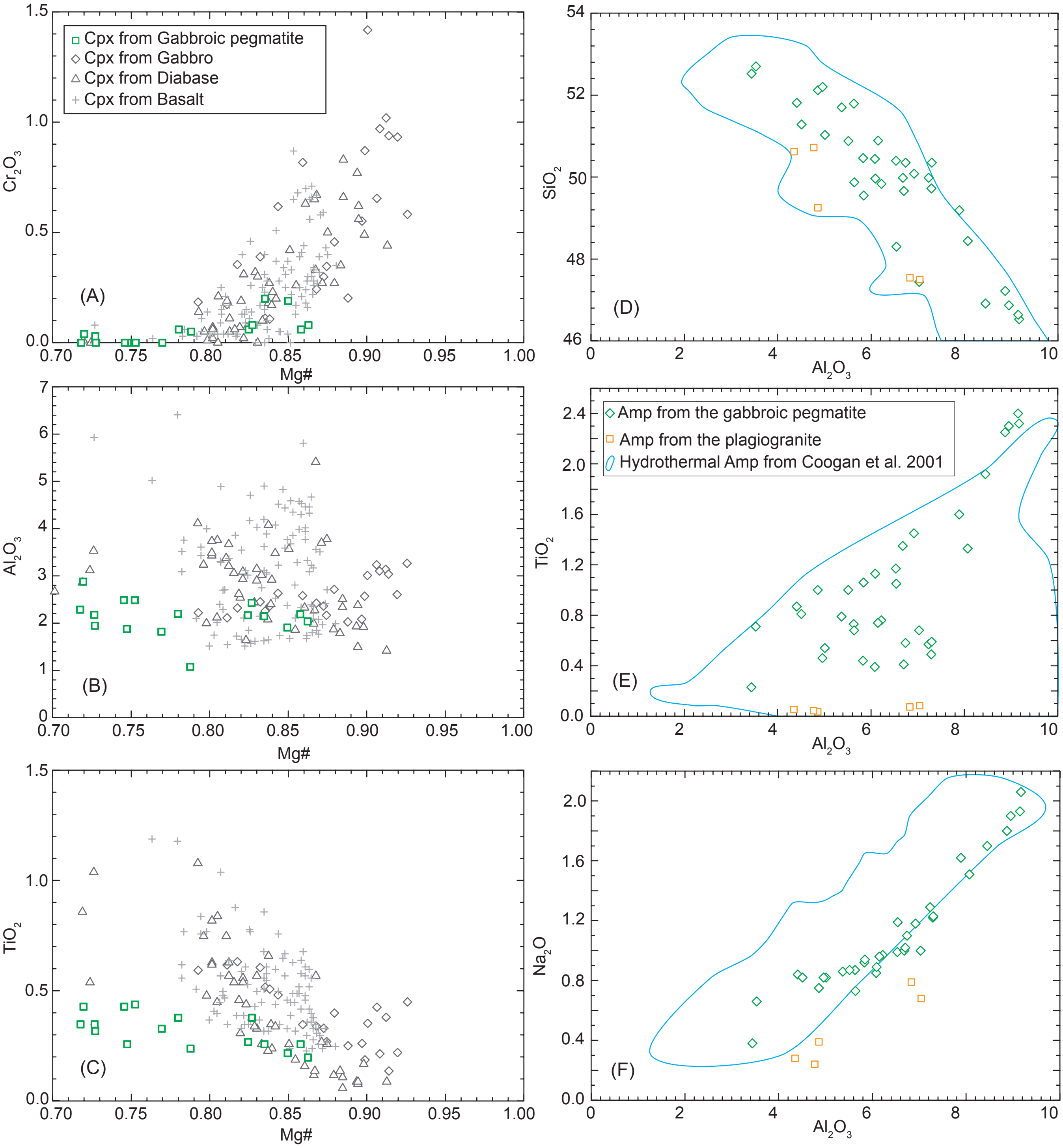
Cpx from Gabbroic pegmatite
Cpx from Gabbro
Cpx from Diabase
Cpx from Basalt
(A)
Cr_2O_3
Mg#
(B)
Al_2O_3
Mg#
(C)
TiO_2
Mg#
(D)
SiO_2
Al_2O_3
Amp from the gabbroic pegmatite
Amp from the plagiogranite
Hydrothermal Amp from Coogan et al. 2001
(E)
TiO_2
Al_2O_3
(F)
Na_2O
Al_2O_3

Figure DR3

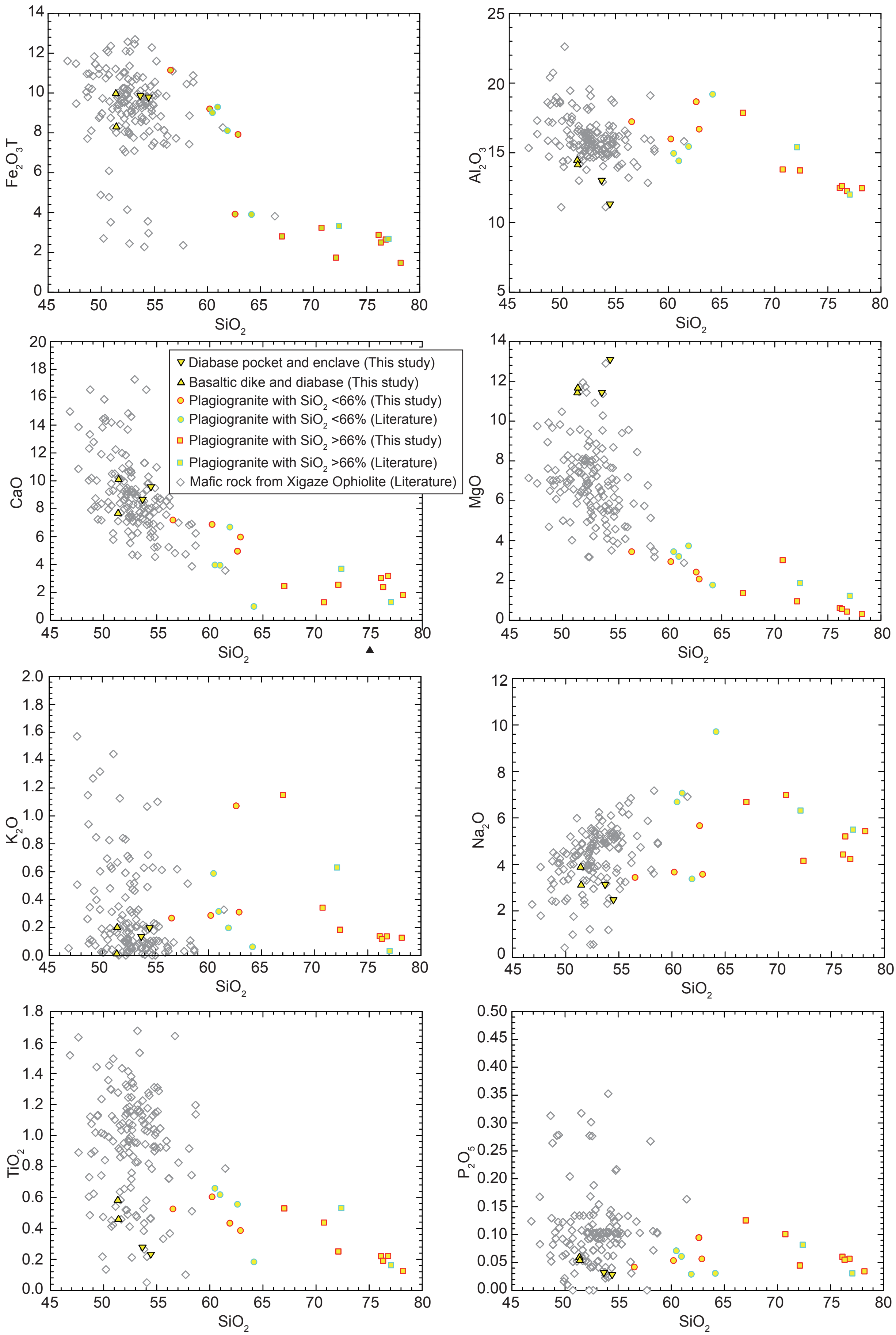

Diabase pocket and enclave (This study)
Basaltic dike and diabase (This study)
Plagiogranite with SiO_2 <66% (This study)
Plagiogranite with SiO_2 <66% (Literature)
Plagiogranite with SiO_2 >66% (This study)
Plagiogranite with SiO_2 >66% (Literature)
Mafic rock from Xigaze Ophiolite (Literature)
Fe_2O_3T
Al_2O_3
CaO
MgO
K_2O
Na_2O
TiO_2
P_2O_5
SiO_2

Figure DR4

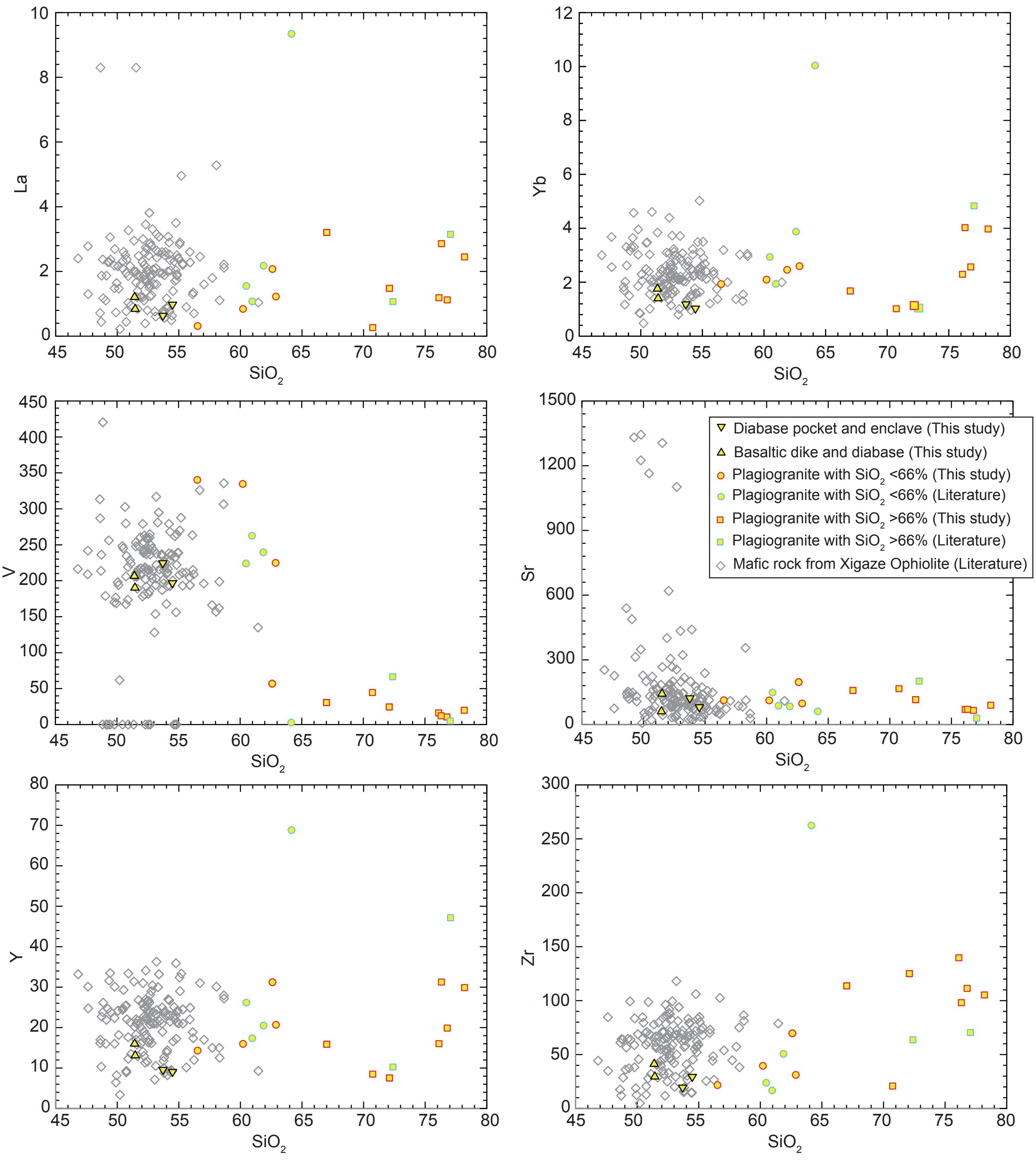

La
Yb
V
Sr
Y
Zr
SiO2
Diabase pocket and enclave (This study)
Basaltic dike and diabase (This study)
Plagiogranite with SiO2 <66% (This study)
Plagiogranite with SiO2 <66% (Literature)
Plagiogranite with SiO2 >66% (This study)
Plagiogranite with SiO2 >66% (Literature)
Mafic rock from Xigaze Ophiolite (Literature)

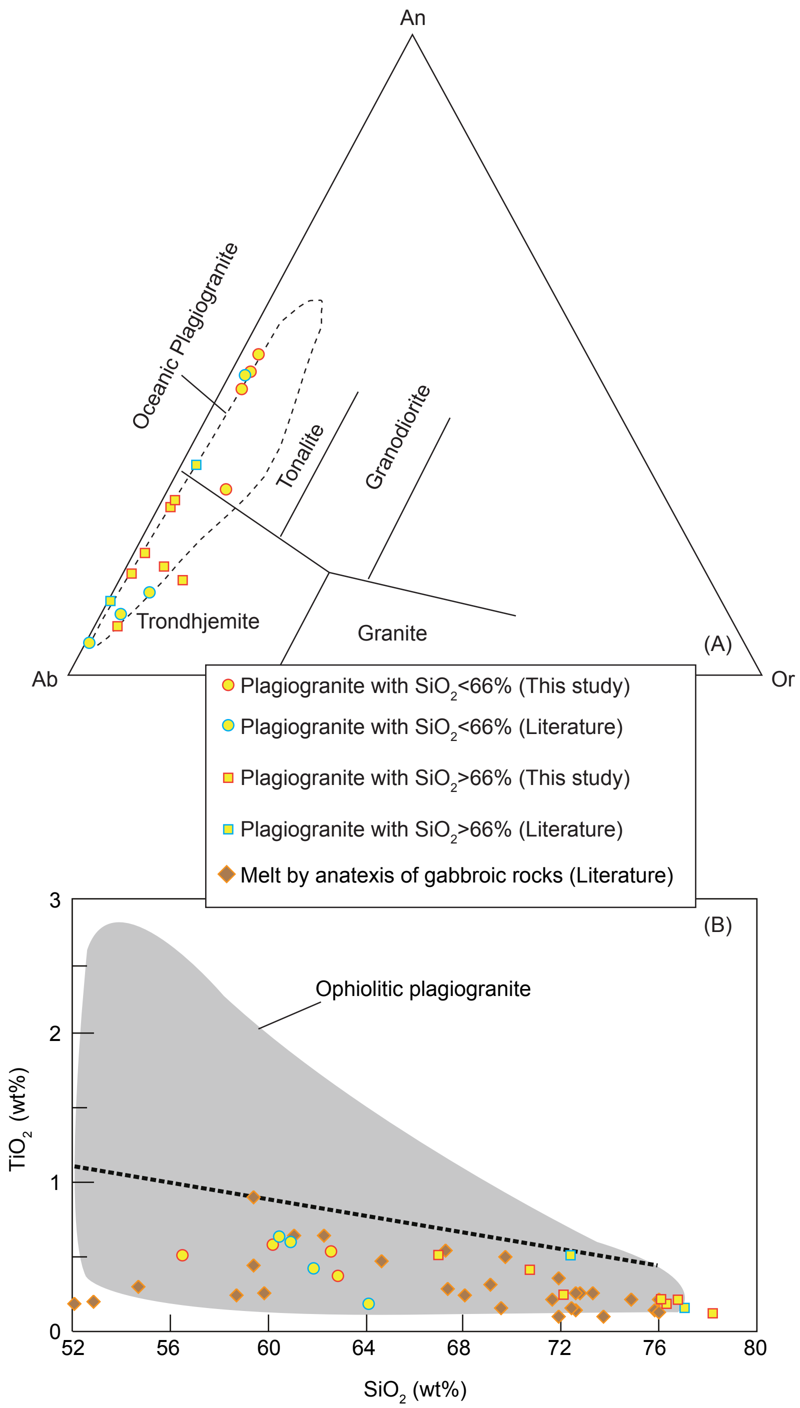
An
Ab
Or
Oceanic Plagiogranite
Tonalite
Granodiorite
Trondhjemite
Granite
(A)
Plagiogranite with SiO2<66% (This study)
Plagiogranite with SiO2<66% (Literature)
Plagiogranite with SiO2>66% (This study)
Plagiogranite with SiO2>66% (Literature)
Melt by anatexis of gabbroic rocks (Literature)
(B)
Ophiolitic plagiogranite
TiO2 (wt%)
SiO2 (wt%)
0
1
2
3
52
56
60
64
68
72
76
80